Versatility of the Curcumin Scaffold: Discovery of Potent and Balanced Dual BACE-1 and GSK-3β Inhibitors

The versatility of the Curcumin Scaffold: Discovery of Potent and Balanced Dual BACE-1 and GSK-3β Inhibitors

Rita Maria Concetta Di Martino,[1] Angela De Simone,[2] Vincenza Andrisano,[2] Paola Bisignano,[3] Alessandra Bisi,[1] Silvia Gobbi,[1] Angela Rampa,[1] Daniel I. Perez,[4] Ana Martinez,[4] Giovanni Bottegoni,[3] Andrea Cavalli,[1,3] Federica Belluti[1]*

[1]Department of Pharmacy and Biotechonology, Alma Mater Studiorum - University of Bologna, Via Belmeloro 6, 40126 Bologna (Italy);

[2]Department for Life Quality Studies, Alma Mater Studiorum - University of Bologna, Corso D'Augusto 237, 47921 Rimini (Italy);

[3]Istituto Italiano di Tecnologia, D3, via Morego 30, 16163 Genova (Italy);

[4]Centro de Investigaciones Biologica, CSIC, Ramiro de Maetzu 9, 28040 Madrid (Spain);

Abstract

Multitarget approaches are gaining ever-increased attention as useful tools to achieve effective disease-modifying drug candidates to treat Alzheimer's disease (AD), a complex and multifactorial malady. The concurrent inhibition of the validated AD targets β-secretase (BACE-1) and glycogen synthase kinase-3β (GSK3-β), by attacking both beta-amyloid and tau protein cascades, has been identified as a promising therapeutic strategy. Here, in the search for novel dual BACE-1 and GSK3-β inhibitors, curcumin was rationally identified as a potential lead compound for the simultaneous inhibition of both targets. Therefore, synthetic efforts were dedicated to obtaining a small library of novel purposely designed curcumin-based analogues. Enzyme inhibition data confirmed our initial hypothesis, as a number of potent and balanced dual-target inhibitors were

obtained. In particular, **2**, **6** and **7** emerged as promising drug candidates endowed with a valuable neuroprotective potential and brain permeability. Notably, for the new compounds the symmetrical β-diketo tautomer and the corresponding keto-enol form were isolated and *in vitro* tested, allowing to gain insight into the key requirements for BACE-1 and GSK3-β inhibition. Further studies, including blood-brain barrier penetration, NQO1 induction and cell viability, demonstrated that these compounds could hold a remarkable AD disease-modifying potential.

Introduction

Alzheimer's disease (AD), the most common form of dementia in industrialized nations among the elderly, is a progressive degenerative disorder, characterized by massive neuronal death and synaptic degeneration, that ultimately leads to the collapse of the neural networks essential for cognition and memory. It is the 6th leading cause of death, currently affecting more than 44 million people worldwide and, due to its debilitating nature, causes an enormous financial and emotional stress on patients and caregivers. Considering that, worldwide, the population is rapidly aging, the number of AD patients is projected to reach 116 million by 2050.[1] The current FDA-approved therapies for moderate to severe AD provide only temporary and incomplete symptomatic relief and represent only a palliative tool by which to slow down the clinical course of the disease.[2] The lack of truly effective drugs is related to the multifactorial nature of the disease, in which several impaired molecular pathways interact in a feed-forward loop.[3,4]

An aberrant protein processing is a distinctive feature of AD, in which amyloid β (Aβ) peptide and abnormally hyperphosphorylated tau protein, upon misfolding, self-assembly and accumulate in the brain as aggregates, namely amyloid senile plaques (SP) and neurofibrillary tangles (NFT), respectively.[5] These assemblies represent the most relevant histopathological hallmarks of the disease and have been considered to play crucial roles in its pathogenesis. Through different molecular mechanisms, these aggregates trigger a cascade of biological processes, among others,

amyloid and tau cascades, respectively, ultimately culminating in neuronal cell death, brain atrophy, and cognitive decline.

Research programs focused on the amyloid cascade still occupy a relevant place, as documented by the substantial number of compounds entered in clinical trials,[6] together with the large amount of published manuscripts. Aβ peptide is generated through a sequential proteolysis of the amyloid β protein precursor (APP) catalyzed by β-and γ-secretases.[7] In this context, the inhibition of β-secretase, an aspartyl protease also known as β-site APP cleaving enzyme (or BACE-1), regulating the first and rate-limiting step of the APP processing, could efficiently block the production of Aβ and of other post-translational products.[8] The highest BACE-1 expression and activity detected in AD patients' brain are consistent with the elevated Aβ levels. The availability of BACE-1 crystal structure greatly enabled the drug development process in this field. This aspartyl protease is characterized by a bilobal structure, the active site is a long cleft for substrate recognition with a flap region that, descending over the top, pins the substrate nearby to two catalytic aspartic residues at the site of bond hydrolysis.[9] Interestingly, a molecular interplay between Aβ and tau in causing synergic toxicity is a recent and intriguing finding, even if the molecular basis of the process still remain to be fully deciphered.[10]

Under normal physiological conditions, tau is associated to microtubules and, preventing their dynamic instability, contributes to morphogenesis of neurons.[11] The strong correlation between tau hyperphosphorylation and AD pathology focuses the attention on tau kinases and, among them, glycogen synthase kinase-3β (GSK-3β), a multi-tasking serine / threonine kinase largely expressed in central nervous system (CNS), proved to play a significant role in regulating tau phosphorylation under both physiological and pathological conditions.[12] In particular, GSK-3β dysregulation is believed to contribute, through a large number of cellular processes, to the etiology of chronic conditions such as diabetes, cancer, and CNS disorders i.e. schizophrenia and AD.[13] GSK-3β induces tau phosphorylation mainly at Ser199, Ser396, Ser413, causes tau disjunction from the microtubules and aggregation as NFT.[14] Over the last decade, the increased interest in GSK-3β

prompted the discovery of a number of inhibitors, based on chemically different molecular scaffolds, and acting with different mechanisms of action, such as ATP competition, allosteric modulation, and enzyme irreversible inhibition.[15] The last two approaches allowed to minimize the undesirable off-target effects. In particular, an irreversible inhibition, by selective targeting of a cysteine residue (Cys199) in the ATP-binding site, has been reported as a promising strategy for obtaining useful pharmacological tools.[16] Interestingly, the cross-talk between GSK-3β and Aβ suggested GSK-3β as molecular link among Aβ and tau. The GSK-3β pathological activation by Aβ, through the prevention of the inhibitory phosphorylation of this kinase, leads to an increment of tau phosphorylation.[17,18] Furthermore, inhibition of this kinase decreases Aβ production and Aβ-induced neurotoxicity by reducing BACE-1 cleavage of APP.[13]

Disease-modifying therapeutics, able to hit the AD underlying physiopathology, would represent an ideal tool to control both onset and progression of the neurodegenerative process.[19,20] Recently, it has become evident that the concurrent modulation of several targets involved in this complex disease could represent an ideal strategy for achieving an effective treatment.[21,22] The idea is to devise multi-target agents that might provide a better efficacy profile, compared with a single-target therapeutic.[23] In this regard, a crucial issue in the drug discovery field is represented by obtaining balanced potency toward the selected targets is a single chemical entity.[24] In this scenario, a multitarget approach, based on the simultaneous inhibition of BACE-1 and GSK-3β disease-modifying AD relevant targets, offers promises to achieve a successful AD treatment.[25] To further corroborate this challenging and still underexplored drug discovery hypothesis, and as continuation of our research studies aimed at the discovery of naturally-inspired compounds as multipotent AD drug candidates, [26-27] we rationally designed a new series of dual BACE-1 and GSK-3β inhibitors based on the curcumin scaffold.

Natural products proved to be an excellent source of lead compounds for drug discovery.[28] These small molecules, synthesized by plant kingdom, are considered as “privileged structures” because they have evolved in the natural selection process to achieve optimal interactions with a number of

biological targets.[29] The polyphenol curcumin (**1a**, Figure 1), 1,7-bis(4-hydroxy-3-methoxyphenyl)-1,6-heptadien-3,5-dione, the primary bioactive compound found in the rhizomes of *Curcuma longa* L.,[30] is one of the most thoroughly investigated natural product, as documented by studies claiming its efficacy and safety for both prevention and treatment of various disorders.[31,32] This pharmacological pleiotropic behaviour has been proposed to be strictly related to its mechanism of action that consists in a synergistic binding to different target proteins involved in related signalling pathways. For instance, molecular basis of curcumin-mediated neuroprotection revealed the participation of a wide range of AD networked pathways, namely aggregation of Aβ and tau proteins, oxidative stress, and neuroinflammation.[33] Moreover, from a medicinal chemistry standpoint, the curcumin pharmacophore proved to be an excellent lead for the design of analogues with improved biological profile.[34]

Several investigations have been focused on curcumin tautomeric behavior, from a theoretical point of view, the solution structure of curcumin has been represented as an equilibrium mixture of the symmetric β-diketo tautomer (**1a**) and the asymmetric keto-enol tautomer (**1b**). More recent theoretical and spectroscopic studies clearly provided evidences that **1b** is the predominant form in a wide range of organic solvents and buffered solutions due to the stabilizing effect of the intramolecular H-bond on the α,γ-unsaturated-keto-enol moiety, property that may play a critical role in determining its affinity to biological targets (Figure 1).[35-36]

Rational design of dual BACE-1 and GSK-3β inhibitors

Notwithstanding the fact that BACE-1 and GSK-3β are structurally unrelated enzymes and greatly differ in both three-dimensional structures and binding site topologies, we rationally envisaged the diarylheptadienone function, main backbone of curcumin, as appropriate structural element for their simultaneous modulation. In particular, the 3,5-dione central core (as β-keto-enol tautomer **1b**) looked to be suitable for the interaction with BACE-1 catalytic dyad (Asp32 and Asp228), whereas the highly electrophilic α,β-unsaturated carbonyl system, a well-known Michael

acceptor system,[37] could covalently interact with a non-conserved cysteine residue of GSK-3β (Cys199).

To substantiate this hypothesis, the interactions of curcumin **1b** with the binding pocket of both targets were investigated by means of docking simulations (Figures 2a and 2b). Figure 2a showed how, in the BACE-1 catalytic pocket, the central core was hydrogen bonded to the crucial Asp32 and Asp228 residues, while the side aryl ring established contacts with Tyr198, Lys224, and Tyr71. Figure 2b reported the predicted binding affinities of **1b** at GSK-3β binding pocket, that were in good agreement with a previously proposed binding mode.[38] In particular, a number of significant interactions were established, among them, the central keto-enol function participated in a H-bond with Tyr134 and Val135, and the two aryl functions contacted Lys85, Glu97, and Arg141, Glu173, respectively.

Furthermore, we tested the naturally occurring curcumin (**1b**) and its simplified analogue bis-demethoxycurcumin (**4**) for their ability to inhibit both BACE-1 and GSK-3β enzymes (Table 1). With regards to BACE-1 inhibition, curcumin resulted in moderate potency, while low-micromolar activity was observed for **4,** confirming previously reported data.[39] In the GSK-3β inhibition assay, both compounds proved to analogously modulate the enzyme (micromolar IC_{50} values). In summary, **4** showed a promising dual BACE-1 / GSK-3β inhibitory profile (2.54 μM and 8.39 μM on BACE-1 and GSK-3β, respectively). Taken together, these initial investigations confirmed the suitability of the curcumin scaffold for the development of effective dual BACE-1 and GSK-3β inhibitors.

To explore the chemical space of the two targets and perform a preliminary structure-activity relationship (SAR) study, a small library of curcumin-based analogues (Figure 1) was designed and synthesized. Different moieties were introduced on the side aryl functions of the main scaffold, while the central heptadienone fragment was retained. The choice of the substituents was mainly addressed to favor the crossing of the blood brain barrier (BBB), as this pharmacokinetic property represents an essential requirement for drugs targeting CNS. The new curcumin-based analogues

(Tables 1 and 2) were primarily screened on BACE-1 and GSK-3β enzymes to determine their inhibitory profiles. Subsequently, for the most promising compounds, in terms of inhibitory activities (high potency against one target or balanced inhibitory profile on both targets), the AD-modifying profile, namely neuroprotection, potential neurotoxicity, and ability to cross the BBB, were also investigated. Analogously, docking simulations were performed, in order to study the general positioning of this new series within the active site of both targets and to assess specific interactions with the residues of the catalytic pockets. To this aim, we selected **8** and **5** as the most potent BACE-1 and GSK-3β inhibitors of the series, respectively, and **2**, **4**, **6**, and **7** as balanced micromolar dualistic inhibitors.

Chemistry

The synthetic route for obtaining the target curcumin-based compounds (**2-8**, **11**, **12**) is outlined in Schemes 1 and 2, applying the Pabon reaction.[40] In summary, pentane-2,4-dione was complexed with B_2O_3 in ethyl acetate (EtOAc) to avoid the methylene-centred reactivity toward the Knoevenagel reaction and to favour the nucleophilic attack at the side methyl groups. The boric complex was then condensed with the suitable aldehyde and then a step-wise addition of tributylborate and *n*-butylamine was carried out. Acidic treatment allowed the complex to dissociate. The synthesis of the asymmetric curcumin-based analogues (**2**, **3**, **6**, **7**) could be performed by condensing two different aldehydes, obtaining thus a complex mixture of compounds, among them the asymmetrical and the two symmetrical curcuminoids, including the semi-reaction (mono-aryl curcumin) products. Consequently, obtaining the desired compounds in a good yield and purity grade requires several purification processes (column chromatography). To avoid this drawback, we performed the synthesis of the asymmetric curcumin analogues (Scheme 1) *via* a two-steps strategy, in which the mono-aryl curcumin synthetic intermediates were first prepared under the classical reaction condition, employing vanillin or 4-benzyloxybenzaldehyde (**17** and 1**8**, respectively). Subsequently, a second Pabon reaction, with a suitable aldehyde, allowed to obtain the desired final compounds. Scheme 2 reports the synthetic one-pot procedure for obtaining the

symmetrical analogues (**4**, **5**, **8**, **11**, **12**). During the course of the Williamson reaction (Scheme 3) of the phenol-key intermediate (**4**) with the selected halides, mixtures of keto-enol and symmetric β-diketo tautomers were obtained (**9**, **15** and **10**, **16**, respectively). The single tautomers were then isolated from the crude reaction by flash column chromatography, and further purified by crystallization from a suitable solvent, thus obtaining the target compounds in high purity grade.

Results and Discussion

BACE-1 and GSK-3β Enzymes Inhibition

BACE-1 inhibition

The ability to inhibit BACE-1 enzyme activity was investigated by means of a biochemical assay performed using the fluorescence resonance energy transfer (FRET) methodology[41] and using curcumin as reference compound. The results are reported in Tables 1 and 2. All the tested compounds **2**-**16**, turned out to effectively inhibit BACE-1, more than **1b** (in our *in vitro* test, it does not inhibit this enzyme up to 3 μM) with IC_{50} ranging from nanomolar to low micromolar values. These good potencies confirmed the suitability of the curcumin main framework to BACE-1 inhibition, substantiating the design rationale for this target, even if the nature of the substituents on the side aryl functions seemed to have an intense effect on activity. The structurally closely related **2** and **3**, bearing the curcumin's 4-hydroxy-3-methoxyphenyl substitution pattern as A ring, and the 4-benzyloxyphenyl and the *para*-tolyl as B ring, respectively, proved to effectively inhibit BACE-1 (IC_{50} values of 0.97 and 0.14 μM, respectively). The corresponding bis-*para*-benzyloxyphenyl symmetrical analogue **8** showed high potency, and, with an IC_{50} value of 40 nM, was the most active compound of the series. A remarkable drop of potency (two orders of magnitude) was observed for the corresponding β-diketo tautomer (**14**). Docked pose of **8** at BACE-1 binding site (Figure 3a) was in good agreement with the reported activity, as the molecule spanned the enzyme active site and the benzyloxy rings pointed toward both the S and the S' subpockets, binding the hydrophobic region described by the side chains of aromatic residues (Tyr198) and the flap region.

From this structure-based docking simulation, it was evident that, to maintain this optimal binding mode, the benzyl rings of **8**-based analogues could only be decorated with small substituents, such as a fluorine atom. The latter, when strategically positioned, have been reported to positively affect the biological profile in terms of enhanced binding interaction, metabolic stability, and selective reactivity[42] allowing the development of effective BACE-1 inhibitors.[43,26] Symmetrically fluorinated **8**-analogues were synthetized and a lower potency (one order of magnitude) relative to **8** was observed for compounds **9** and **10** (2,4-di-F and 3,5-di-substituted analogues, IC_{50} = 0.40 and 0.39 μM, respectively), and a further drop in activity was documented for **11** and **12** (4-F and 3-F substituted analogues, IC_{50} = 1.04 and 1.08 μM, respectively). For this subset, the corresponding β-diketo tautomers of the di-fluorinated **9** and **10 (15** and **16)**, as the most active compounds of the series, showed only a moderate decrement of activity. When one or both benzyloxy moieties of **8** were replaced by methoxy and hydroxy (**4**-**7**), low micromolar inhibitory potencies were observed. Analogously to **14**, the **5**-β-diketo tautomer (**13**) was less active than the corresponding keto-enol. Taken together, these data pointed out that the structural modifications on **8** had, in general, detrimental effects on BACE-1 inhibiting activity.

GSK-3β Inhibition

A luminescent assay was employed for the evaluation of the GSK-3β inhibitory potency.[44] The curcumin-based analogues (**2**-**16**) showed a narrower GSK-3β inhibition range compared to that observed for BACE-1 (IC_{50} values from 0.53 to 16.99 μM). All the tested compounds showed micromolar activities, except for the *para*-methoxy substituted **5**, with an IC_{50} value of 0.53 μM, that proved to be the most active in the series, more potent than **1b** (IC_{50} = 17.95 μM) and **4** (IC_{50} = 8.39 μM). Good GSK-3β inhibition was also obtained with the replacement of a side aryl ring of curcumin with a *para*-benzyloxyphenyl and a *para*-tolyl functions (**2** and **3**, IC_{50} = 0.90 and 2.09 μM, respectively). Moreover, **8**, **6**, and **7**, all bearing a *para*-benzyloxyphenyl moiety, showed similar inhibitory potencies (around 2 μM). A lowered inhibitory potency was observed for the **8**-

based fluorinated subset (IC_{50} values ranging from 8.30 to 16.99 μM) that proved to be slightly more active or as active as **1b**. Concerning the β-diketo tautomers, only for **13** a notable divergence in activity was observed with respect to the keto-enol counterpart, for the other compounds of this series bearing *para*-benzyloxyphenyl groups (**14**, **15** and **16)** only a moderate decrease in activity was observed. In light of these results, among the tested compounds **8** and **5** proved to be the most potent BACE-1 and GSK-3β inhibitors, respectively. A well-balanced dual low-micromolar inhibition profile was observed for **2**, **6** and **7**, thus offering promises for gaining ground in the development of curcumin-based multitarget drug candidates for AD treatment.

Computer-assisted studies

Aimed at gaining insight into the molecular determinants of the curcumin-based analogues involved in effective interactions with BACE-1 and GSK-3β binding sites, docking studies were performed on **8**, **5**, as highly active principally on one of the two targets, and on **6** and **7** as balanced inhibitors.

Docking studies on BACE-1

Docking studies at the binding site of BACE-1 were in line with the experimental results, with **8** displaying the most potent activity, thanks to its ability to establish a direct interaction with the catalytic dyad and, at the same time, to concurrently engage both the S and the S' sub-sites (Figure 3a).[45] In particular, this compound with the benzyloxy substituent showed to contact the side chains of Trp197, Tyr198, Lys224 at P_3 and the side chains of Lys107 and Ile110 at P_3'. According to the proposed binding mode, for the compounds with less hindering side functions (**5** and **6**, and **7**, Figures 3b, 3c, and 3d, respectively**)** the incapability of contacting all sub-sites was observed, this could explain the decrease in potency (low-micromolar) with respect to that of **8**. Notably, the *para*-hydroxyl group of **7** was likely interacting with the backbone of Lys107 or Phe108, forming an additional H-bond interaction.

Docking studies on GSK-3β

Docking studies at the binding site of GSK-3β turned out to be in fairly good agreement with the experimental activities. All compounds bind at the hinge region of the ATP binding site. However, due to the bulky nature of the side substituent, **8** was not able to adopt a bound conformation that could favor strong hydrogen bond interactions with the backbones of Asp133 and Tyr134 (Figure 4a). The same behavior was also observed for the less hindered **6** (Figure 4c). Conversely, **7**, (Figure 4d) by means of the hydroxy group, was able to establish stronger hydrogen bond interactions at the hinge region, and to contact the residues forming the kinase conserved salt bridge (Lys85 and Glu97). The benzyloxy substituent protrudes toward the bulk of the solvent, possibly establishing stacking interactions with the side chain of Arg141. Due to its smaller size, **5** can be entirely lodged within the binding pocket, without protruding in the solvent or creating steric hindrance in the salt bridge region, thus displaying the most suitable interaction with the hinge (Figure 4b).

Taking into account the frequently claimed strong correlation among compound's reactivity and bioactivity, and the highly and well established electrophilic properties of the curcumin pharmacophore, a covalent docking was accomplished in which a thia-Michael reaction occurred by nucleophilic attack of GSK-3β Cys199 residue on the reactive α,β-unsaturated carbonyl function of **5** (Figure 5). It can be speculated that specific non-covalent interactions of the molecule with the binding pocket of the target are critical for the optimal orientation of the electrophile pharmacophore toward a specific protein nucleophile residue, thus increasing the speed and selectivity of the interaction (covalent bond).

Thiol trapping assay

To support the covalent docking study, a spectroscopic ^{1}H-NMR-based thiol trapping assay was performed. This procedure has been described for several electrophilic compounds, among them curcumin,[46] that was reported to irreversibly and quickly react with cysteamine in DMSO-*d*6 to afford the corresponding bis-1,7-thia-Michael adduct, as documented by the disappearance of the

AB olefinic signals on the ^{1}H-NMR spectra.[47] Compound **5** underwent a thiol-trapping reaction by employing a mixture of **5** / cysteamine in a 1:2 stoichiometric ratio,[46] affording the corresponding thia-Michael adduct in very short time as documented in Figure 6. Analogously, competitive experiments were also carried out on **2**, **8** and **6**; longer times of reaction were observed, with respect to **5,** with the following reactivity order: **5** > **2** > **6** ~ **8**, suggesting a potential detrimental effect on reactivity elicited by the benzyloxy function, partially compensated by the presence of the 4-OH, 3-OCH_3-aryl ring (**2**).

Chemical Stability Studies

A number of studies provided evidences about the curcumin's poor stability in aqueous solutions at physiological pH and several degradation products were identified.[48, 49] The chemical stability of keto-enol **5** and its β-diketo tautomeric counterpart, together with their potential interconversion, were studied by RP-HPLC. For **5**, in the working conditions, no degradation or tautomeric conversion was observed. On the contrary, by analyzing the DMSO solution of **13** the formation of a degradation product was noted. This derivative was separated from the mixture and its structure was determined by ^{1}H-NMR spectroscopy and (ESI)–MS as the diketene derivative (1*E*,4*E*-1,5-bis-4-methoxyphenylpenta-1,4-dien-3-one), endorsing a reported curcumin's behaviour.[49] On the contrary, **14** and the fluorinated-benzyloxy derivatives, obtained with similar synthetic route as **13**, showed a good chemical stability, and no degradation product was observed during the purification procedure. The presence of these benzyloxy functions seemed to strongly increase compound stability.

Blood-Brain Barrier (BBB) Permeation

One of the main obstacles for the treatment of the diseases of the CNS is drug's penetration into BBB at therapeutic concentrations. The BBB is a complex interface between blood and the CNS that strictly controls exchanges between the blood and brain compartments.[50] This barrier is composed by endothelial cells with tight junctions that protect the brain from endogenous materials

which could damage brain tissues.[51] The majority of CNS drugs enter the brain by transcellular passive diffusion, due to the tight junction structure and limited transport pathways. In early drug discovery stage, evaluation of ADME (Absorption, Distribution, Metabolism, Excretion) properties is of crucial importance to reduce attrition in the development process. Parallel Artificial Membrane Permeability Assay (PAMPA), is a high throughput technique developed to predict passive permeability through biological membranes. As curcumin and its metabolites were reported to have poor BBB permeability,[52] it seemed to be significant to evaluate the new derivatives for their impact on BBB crossing. Thus, the capacity of the selected candidates (**2**, **3**, **5**, **7**, **8**) to penetrate into the CNS was examined through the PAMPA-BBB method described by Di et al,[53] using curcumin (**1b**) as standard. The *in vitro* permeabilities (Pe) values were determined, expressed as 10^{-6} cm·s^{-1}, and reported in Table 3. In the lights of the guidelines previously established for the prediction of the BBB permeation,[54] compounds with a Pe value superior than 4.22 10^{-6} cm·s^{-1} could be considered as capable of crossing the BBB and classified as CNS +; a border-line profile was reported as CNS + / CNS -. Based on the results, we can consider compounds **2**, **3**, **6** and **7** able to efficiently cross the BBB by passive permeation, while **5** and **8** showed a border-line behavior.

Neuroprotection

The neuroprotective potential was also investigated for some selected compounds by evaluating: i) antioxidant properties, ii) induction of the detoxifying enzyme NAD(P)H:quinone oxidoreductase (NQO1), iii) cell viability. Curcumin (**1b**) was employed as reference compound.

i) **Antioxidant properties.** Oxidative stress has been recognized as a common pathological feature in AD. It is substantially produced by reactive radical species, among others reactive oxygen species (ROS), together with loss of function of many antioxidant defense enzymes that cause imbalance between the formation of cellular oxidants and the antioxidative processes.[55] Compounds able to inactivate these entities could offer promises for a valuable therapeutic efficacy. The ability of the selected curcumin-based derivatives **2**, **3** and **8** to protect from oxidative stress was studied on

T67 cells, by evaluating their ROS scavenging ability after exposure to 100 μM *tert*-butyl hydroperoxide (TBH) at the fixed concentration of 10 μM (Figure 7). The results showed that **2** maintained a moderate scavenging activity, slightly lower than curcumin (P = 0.005 for curcumin *vs*. TBH and P = 0.08 for **2** *vs*. TBH), while **3** and **8**, although displaying the same mean value, show a higher standard deviation that makes them not significant. The lack of scavenging activity observed for **3** suggested that this property could not only be ascribed to the presence of the 3-OCH_3, 4-OH-aryl function.

ii) **NQO1 induction.** Human NQO1, a flavoprotein constitutively expressed in several tissues and organs, among which the brain, exerts antioxidant effect by catalyzing the reduction of quinones to hydroquinones and by scavenging superoxide molecules.[56] In AD, as a result of a defense mechanism against an increased oxidative stress, the levels of this phase 2 cytoprotective enzyme were found to be remarkably increased. Interestingly, an elevated expression of this enzyme has also been proposed as a first indicator of the patology.[57] Its induction may correlate with a protective role by allowing to delay the progression of the malady. As curcumin itself was demonstrated to effectively induce NQO1,[58] a set of representative derivatives (**2-8**) were selected to be tested on NQO1 induction potential. As shown in Figure 8, the tested compounds proved to be NQO1 inducers. In particular, **8** and **4** were as active as curcumin, while higher activities were observed for **2**, **3** and **6**. Notably, this effect has recently been demonstrated to slow the Aβ-induced neurodegeneration in mice.[59]

iii) **Neuronal Cell Toxicity.** Cytotoxic effects, in several *in vitro* or *in vivo* models, have been reported for curcumin.[60] The neurotoxic potential was thus examined for some selected compounds, namely **2-8.** Cells were exposed to compound concentrations ranging from 0 to 20 μM, for a 24 h period of time and cell viability was measured by the MTT test, with **1b** as reference compound. As shown in Figure 9, in the experimental conditions, increasing the concentration of the tested compound, no remarkable decrease of cell viability was observed. In particular, **4** and **7** showed moderate toxicity at 20 μM concentration, comparable to that of **1b**, that for **7** was dose-dependent.

The remaining compounds did not show any apparent cytotoxic effects at these concentrations. The potential toxicity of **5**, **4** and **6** was assayed only at the concentration of 10 μM after 24 hours of incubation and the results confirmed the absence of any apparent cytotoxic effect.

Conclusion

The complex pathological mechanisms of AD directed attention to polypharmacological strategies and multi-target drugs that, acting on several targets involved in the disease, could offer promises for obtaining improved effectiveness compared to single-target drugs. In this scenario, BACE-1 and GSK3-β emerged as AD validated targets. The curcumin pharmacophore, in its β-keto-enol form, was rationally envisaged as a dualistic BACE-1 and GSK3-β inhibitor as it encompassed the structural features needed for inhibition of both targets. Efforts addressed to rationally design and synthesize a small library of curcumin-based analogues allowed to obtain useful chemical probes exploring the chemical space of these structurally unrelated targets. The keto-enol tautomer form appeared to be an essential chemical feature for good chemical stability and inhibitory potency. Among the keto-enol series, some balanced and effective (low-micromolar) dual-target modulators endowed with a promising neuroprotective potential and favourable pharmacokinetic behaviour were discovered (**2**, **6,** and **7**). In particular compound **2**, lacking neurotoxic effects, and with a bland antioxidant effect, clearly emerged as disease-modifying drug candidate for the treatment of AD. Meanwhile, **8** and **3** turned out to be very potent inhibitors of only BACE-1 (nanomolar and sub-micromolar potencies, respectively), with a unbalanced potencies of one or two orders of magnitude with respect to GSK-3β inhibition (low- micromolar activities). A reduced gap from a dualistic profile was shown for **5**. In light of these findings, in this study, several curcumin-based analogues were identified as valuable candidates that deserve attention to be optimized and transformed into potent dual-target inhibitors with improved neuroprotective and pharmacokinetic properties. Moreover, this class of compounds could hold a remarkable potential as disease-modifying agents for AD cure.

EXPERIMENTAL SECTION

Chemistry. General Procedures. Starting materials, unless otherwise specified in the Experimental Section, were used as high-grade commercial products. Solvents were of analytical grade. Melting points were determined in open glass capillaries, using a Büchi apparatus and are uncorrected. ^{1}H NMR and ^{13}C NMR spectra were recorded on Varian Gemini and chemical shifts are reported as parts per million (ppm δ value) relative to the peak for tetramethylsilane (TMS) as internal standard. Standard abbreviations indicating spin multiplicities are given as follows: s (singlet), d (doublet), t (triplet), br (broad), q (quartet) or m (multiplet). Mass spectra were recorded on a Waters ZQ 4000 apparatus operating in electrospray mode (ES). Chromatographic separations were performed on silica gel columns using the flash method (Kieselgel 40, 0.040-0.063 mm, Merck). Reactions were followed by thin layer chromatography (TLC) on precoated silica gel plates (Merck Silica Gel 60 F254) and then visualized with a UV lamp. Satisfactory elemental analyses were obtained for all new compounds, confirming >95 % purity. Compounds were named following IUPAC rules as applied by Beilstein-Institute AutoNom (version 2.1), a PC-integrated software package for systematic names in organic chemistry.

Pabon reaction: General Synthetic Procedure for Compounds 2-8, 17, 18. To a stirred solution of pentane-2,4-dione (1.00 mmol) in EtOAc (1.0 mL), B_2O_3 (1.0 molar equiv) was added, and the suspension was stirred for 30 min at 80 °C before addition of a solution of the appropriate aldehyde/s, (0.9 molar equiv for monoaryl or 1.8 molar equiv for bi-aryl curcumin derivatives), tri-*n*-butyl borate (2.0 molar equiv for monoaryl or 4.0 molar equiv for bi-aryl curcumin derivatives), in EtOAc (0.5 mL). The reaction mixture was stirred at 80°C for 30 min, then a solution of *n*-butylammine (0.4 molar equiv in 1.0 mL of EtOAc) was added over a period of 15 min. The mixture was heated to 80 °C for 8 h and then, after cooling to r.t., it was acidified with 0.5 N HCl (30 mL) and then stirred at 80 °C for 30 min. The organic phase was separated and the aqueous layer was extracted with EtOAc (3 x 10 mL). The combined organic layers were sequentially

washed with saturated aqueous $NaHCO_3$ and brine, dried over Na_2SO_4, filtered, and concentrated under reduced pressure. The crude residue was purified by flash column chromatography using a mixture of petroleum ether / ethyl acetate (PE / EtOAc) as eluent, followed by crystallization from suitable solvent.

3*Z*,5*E*-4-hydroxy-6-(4-hydroxy-3-methoxyphenyl)hexa-3,5-dien-2-one (17). Reaction of pentane-2,4-dione (1.00 g, 10.00 mmol), B_2O_3 (0.70 g, 10.00 mmol), and vanillin (1.37 g, 9.00 mmol), in EtOAc (15.0 mL), gave a crude that was purified by flash chromatography (PE / EtOAc, 9.75:0.25), yellow powder, 55 % yield, mp 144-146 °C (EtOH). ^{1}H NMR (400 MHz, $CDCl_3$): δ 2.16 (s, 3H, CH_3), 3.94 (s, 3H, OCH_3), 5.40 (br, 1H, OH), 5.63 (s, 1H, keto-enol-CH), 6.33 (d, 1H, *J* = 16.0 Hz, CH=CH), 6.92 (d, 1H, *J* = 8.0 Hz, H-5), 7.02 (d, 1H, *J* = 1.8 Hz, H-2), 7.09 (dd, 1H, *J* = 8.0 and 1.8 Hz, H-6), 7.53 (d, 1H, *J* = 16.0 Hz, CH=CH). Analytical data of this intermediate are in good agreement with the literature data.[61]

3*Z*,5*E*-6-(4-benzyloxyphenyl)-4-hydroxyhexa-3,5-dien-2-one (18). Reaction of pentane-2,4-dione (1.00 g, 10.00 mmol), B_2O_3 (0.70 g, 10.00 mmol), and 4-benzyloxybenzaldehyde (2.04 g, 9.00 mmol) gave a crude that was purified by flash chromatography (PE / EtOAc, 9.95:0.05), yellow powder, 65 % yield, mp 121-122 °C (DCM / EP). ^{1}H NMR (400 MHz, $CDCl_3$): δ 2.18 (s, 3H, CH_3), 5.20 (s, 2H, OCH_2), 5.61 (s, H, keto-enol-CH), 6.33 (d, 1H, *J* = 16.0 Hz, CH=CH), 6.94 (d, 2H, *J* = 8.2 Hz, Ar), 7.40-7.45 (m, 5H, Bz), 7.53 (d, 2H, *J* = 8.2 Hz, Ar), 7.53 (d, 1H, *J* = 16.0 Hz, CH=CH).

1E,4*Z*,6*E*-7-(4-benzyloxyphenyl)-5-hydroxy-1-(4-hydroxy-3-methoxyphenyl)hepta-1,4,6-trien-3-one (2). Reaction of **17** (1.17 g, 5.00 mmol), B_2O_3 (0.35 g, 5.00 mmol), and 4-benzyloxybenzaldehyde (0.95 g, 4.50 mmol), gave a crude product that was purified by flash chromatography (PE / EtOAc, 9:1), orange-yellow powder, 44 % yield, mp 169-170 °C (EtOH). ^{1}H-NMR (400 MHz, $CDCl_3$): δ 3.96 (s, 3H, OCH_3), 5.19 (s, 2H, OCH_2), 5.76 (s, 1H, keto-enol-CH),

6.45 (d, 2H, *J* = 16.0 Hz, CH=CH), 6.94 (d, 1H, *J* = 8.4 Hz, H-5), 6.98 (d, 2H, *J* = 8.4 Hz, Ar), 7.07 (d, 1H, *J* = 1.8 Hz, H-2), 7.12 (dd, 1H, *J* = 1.8 and 8.4 Hz, H-6), 7.40-7.45 (m, 5H, Bz), 7.53 (d, 2H, *J* = 8.4 Hz, Ar), 7.60 (d, 2H, *J* = 16.0 Hz, CH=CH). ^{13}C-NMR (101 MHz, $CDCl_3$): δ 55.70, 70.44, 103.56, 111.78, 115.81, 116.37 (2C), 123.18, 123.21, 127.58, 128.17 (3C), 128.32 (2C), 128.50 (2C), 129.01, 129.33, 137.27, 140.41 (2C), 148.50, 149.52, 160.78, 186.65 (2C). ESI-MS (*m/z*): 451 (M + Na).

1*E*,4*Z*,6*E*-5-hydroxy-1-(4-hydroxy-3-methoxyphenyl)-7-p-tolylhepta-1,4,6-trien-3-one (3). Reaction of **17** (1.17 g, 5.00 mmol), B_2O_3 (0.35 g, 5.00 mmol), and 4-methylbenzaldehyde (0.53 mL, 4.50 mmol) gave a crude that was purified by flash chromatography (PE / EtOAc, 9:1), orange-yellow powder, 36 % yield, mp 136-138 °C (EtOH). ^{1}H-NMR (400 MHz, $CDCl_3$): δ 2.38 (s, 3H, CH_3), 3.95 (s, 3H, OCH_3), 5.81 (s, 1H, keto-enol-CH), 6.49 (d, 1H *J* = 15.8 Hz, CH=CH), 6.60 (d, 1H, *J* = 15.8 Hz, CH=CH), 6.94 (d, 1H, *J* = 8.2 Hz, H-5), 7.06 (d, 1H, *J* = 1.8 Hz, H-2), 7.13 (dd, 1H, *J* = 1.8 and 8.2 Hz, H-6), 7.20 (d, 2H, *J* = 8.0 Hz, Ar), 7.46 (d, 2H, *J* = 8.0 Hz, Ar), 7.59 (d, 1H, *J* = 15.8 Hz, CH=CH), 7.63 (d, 1H, *J* = 15.8 Hz, CH=CH). ^{13}C-NMR (101 MHz, $CDCl_3$) δ 21.04, 55.70, 107.59, 112.88, 116.00, 121.46, 121.87, 126.70, 127.42 (2C), 129.27 (2C), 130.94, 134.09, 141.23 (2C), 137.91, 148.50, 150.23, 183.70 (2C). ESI-MS (*m/z*): 359 (M + Na).

1*E*,4*Z*,6*E*-1-(4-benzyloxyphenyl)-5-hydroxy-7-4-methoxyphenylhepta-1,4,6-trien-3-one (6). Reaction of **18** (1.47 g, 5.00 mmol), B_2O_3 (0.35 g, 5.00 mmol), and 4-methoxylbenzaldehyde (0.53 mL, 4.50 mmol) gave a crude that was purified by flash chromatography (PE / EtOAc, 4:1), light orange-yellow powder, 48 % yield, mp 135-137 °C (DCM / EP). ^{1}H-NMR (400 MHz, $CDCl_3$): δ 3.86 (s, 3H, OCH_3), 5.12 (s, 2H, OCH_2), 5.80 (s, 1H, keto-enol-CH), 6.51 (d, 2H, *J* = 15.6 Hz, CH=CH), 6.93 (d, 2H, *J* = 8.0 Hz, Ar), 7.00 (d, 2H, *J* = 8.0 Hz, Ar), 7.40-7.45 (m, 5H, Bz), 7.52 (d, 4H, *J* = 8.0 Hz, Ar), 7.63 (d, 2H, *J* = 15.6 Hz, CH=CH). ^{13}C-NMR (101 MHz, $CDCl_3$): δ 55.41, 70.54, 114.68, 114.45 (2C), 115.30 (2C), 122.03, 127.80 (2C), 128.10 (2C), 128.50, 128.99 (2C),

129.79, 129.93 (4C), 137.02, 140.25 (2C), 160.73, 161.01, 183.49 (2C). ESI-MS (*m/z*): 435 (M + Na).

1*E*,4*Z*,6*E*-1-(4-benzyloxyphenyl)-5-hydroxy-7-4-hydroxyphenylhepta-1,4,6-trien-3-one (7). Reaction of **18** (1.47 g, 5.00 mmol), B_2O_3 (0.35 g, 5.00 mmol), and 4-hydroxylbenzaldehyde (0.56 g, 4.50 mmol) gave a rude that was purified by flash chromatography (PE / EtOAc, 9:1), yellow powder, 42 % yield, mp 189-191 °C (EtOH). ^{1}H-NMR (400 MHz, $CDCl_3$): δ 5.11 (s, 2H, OCH_2), 5.78 (s, 1H, keto-enol-CH), 6.49 (d, 1H, *J* = 16.0 Hz, CH=CH), 6.50 (d, 1H, *J* = 15.6 Hz, CH=CH), 6.85 (d, 2H, *J* = 8.0 Hz, Ar), 7.00 (d, 2H, *J* = 8.8 Hz, Ar), 7.40-7.45 (m, 5H, Bz), 7.47 (d, 2H, *J* = 8.0 Hz, Ar), 7.51 (d, 2H, *J* = 8.8 Hz, Ar), 7.61 (d, 1H, *J* = 15.6 Hz, CH=CH), 7.62 (d, 1H, *J* = 15.6 Hz, CH=CH). ^{13}C-NMR (101 MHz, $CDCl_3$): δ 70.70, 114.81, 115.70 (2C), 116.53 (2C), 122.57, 127.98 (2C), 128.21 (2C), 128.29, 129.04 (2C), 129.89, 130.06 (4C), 136.87, 140.74 (2C), 160.80, 161.00, 183.58 (2C). ESI-MS (*m/z*): 421 (M + Na).

1*E*,4*Z*,6*E*-5-hydroxy-1,7-bis-4-hydroxyphenylhepta-1,4,6-trien-3-one (4). Reaction of pentane-2,4-dione (1.00 g, 10.00 mmol), B_2O_3 (0.70 g, 10.00 mmol) and 4-hydroxybenzaldehyde (2.24 g, 18.00 mmol) gave a crude that was purified by flash chromatography (PE / EtOAc, 7:3), red-orange powder, 88 % yield, mp 228-230 °C (EtOH). ^{1}H-NMR (400 MHz, Acetone-d_6): δ 5.99 (s, 1H, keto-enol-CH), 6.67 (d, 2H, *J* = 15.8 Hz, CH=CH), 6.91 (d, 4H, *J* = 8.6 Hz, Ar), 7.57 (d, 4H, *J* = 8.6 Hz, Ar), 7.61 (d, 2H, *J* = 15.8 Hz, CH=CH). ^{1}H-NMR (400 MHz, DMSO): δ 6.22 (s, 1H, keto-enol-CH), 6.82 (d, 2H, *J* = 16.4 Hz, CH=CH), 6.98 (d, 4H, *J* = 8.4 Hz, Ar), 7.25 (d, 4H, *J* = 8.4 Hz, Ar), 7.35 (br, 1H, OH), 7.62 (d, 2H, *J* = 16.4 Hz, CH=CH), 9.7 (br, 2H, OH).[62] ^{13}C-NMR (101 MHz, Acetone-d_6): δ 114.00, 116.50 (4C), 122.86, 127.93 (2C), 129.71, 130.01 (4C), 141.08 (2C), 161.07 (2C), 183.50 (2C). ESI-MS (*m/z*): 331 (M + Na).

1*E*,4*Z*,6*E*-5-hydroxy-1,7-bis-4-methoxyphenylhepta-1,4,6-trien-3-one (5). Reaction of pentane-2,4-dione (1.00 g, 10.00 mmol), B_2O_3 (0.70 g, 10.00 mmol), and 4-methoxybenzaldehyde (2.19 mL, 18.00 mmol) gave a crude that was purified by flash chromatography (PE / EtOAc, 9:1)

yellow powder, 87 % yield, mp 110-112 °C (DCM / PE). ^{1}H-NMR (400 MHz, $CDCl_3$): δ 3.86 (s, 6H, OCH_3), 5.79 (s, 1H, keto-enol-CH), 6.51 (d, 2H, *J* = 15.6 Hz, CH=CH), 6.93 (d, 4H, *J* = 7.2 Hz, Ar), 7.52 (d, 4H, *J* = 7.2 Hz, Ar), 7.63 (d, 2H, *J* = 15.6 Hz, CH=CH). ^{1}H-NMR (400 MHz, DMSO): δ 3.80 (s, 6H, OCH_3), 6.09 (s, 1H, keto-enol-CH), 6.79 (d, 2H, *J* = 15.6 Hz, CH=CH), 7.00 (d, 4H, *J* = 8.4 Hz, Ar), 7.59 (d, 2H, *J* = 15.6 Hz, CH=CH), 7.68 (d, 4H, *J* = 8.4 Hz, Ar). ^{13}C-NMR (101 MHz, $CDCl_3$): δ 55.38 (2C), 113.75, 114.37 (4C), 121.80, 127.80 (2C), 129.51, 129.75 (4C), 140.09 (2C), 161.25 (2C), 183.33 (2C). ^{13}C-NMR (101 MHz, DMSO): δ 55.38 (2C), 101.43, 114.52 (4C), 121.82 (2C), 127.33 (2C), 130.18 (4C), 140.05 (2C), 161.09 (2C), 183.12 (2C). ESI-MS (*m/z*): 359 (M + Na).

1*E*,4*Z*,6*E*-1,7-bis-4-benzyloxyphenyl-5-hydroxyhepta-1,4,6-trien-3-one (8). Reaction of pentane-2,4-dione (1.00 g, 10.00 mmol), B_2O_3 (0.70 g, 10.00 mmol), and 4-benzyloxybenzaldehyde (3.80 g, 18.00 mmol) gave a crude that was purified by flash chromatography (PE / EtOAc, 9:1), yellow powder, 87 % yield, mp 161-162 °C (DCM / PE). ^{1}H-NMR (400 MHz, $CDCl_3$): δ 5.11 (s, 4H, OCH_2), 5.78 (s, 1H, keto-enol-CH), 6.50 (d, 2H, *J* = 16.0 Hz, CH=CH), 6.99 (d, 4H, *J* = 8.4 Hz, Ar), 7.40-7.44 (m, 10H, Bz), 7.51 (d, 4H, *J* = 8.4 Hz, Ar), 7.62 (d, 2H, *J* = 16.0 Hz, CH=CH). ^{1}H-NMR (400 MHz, DMSO): δ 5.17 (s, 4H, OCH_2), 6.09 (s, 1H, keto-enol-CH), 6.79 (d, 2H, *J* = 16.4 Hz, CH=CH), 7.08 (d, 4H, *J* = 8.4 Hz, Ar), 7.40-7.43 (m, 10H, Bz), 7.59 (d, 4H, *J* = 8.4 Hz, Ar), 7.68 (d, 2H, *J* = 15.6 Hz, CH=CH). ^{13}C-NMR (101 MHz, $CDCl_3$): δ 70.44 (2C), 115.61 (5C), 122.27, 127.79 (2C), 127.81 (2C), 128.39 (2C), 128.50 (2C), 128.98 (2C), 129.00 (2C), 130.07, 130.12 (4C), 136.80 (2C), 140.41 (2C), 160.78 (2C), 183.67 (2C). ESI-MS (*m/z*): 511 (M + Na).

1*E*,4*Z*,6*E*-1,7-bis-4-(4-fluorobenzyloxyphenyl)-5-hydroxyhepta-1,4,6-trien-3-one (11). Reaction of pentane-2,4-dione (0.50 g, 5.00 mmol), B_2O_3 (0.35 g, 5.00 mmol), and 4-(4-fluorobenzyloxybenzaldehyde **19** (2.07 g, 9.00 mmol) gave a crude that was purified by flash chromatography (PE / EtOAc, 9:1), yellow solid, 31 % yield, mp 210-212 °C. ^{1}H-NMR (400 MHz, $CDCl_3$): δ 5.06 (s, 4H, OCH_2), 5.78 (s, 1H, keto-enol-CH), 6.50 (d, 2H, *J* = 15.6 Hz, CH=CH), 6.98

(d, 4H, *J* = 8.8 Hz, Ar), 7.09-7.13 (m, 4H, Ar), 7.41-7.44 (m, 4H, Ar), 7.51 (d, 4H, *J* = 8.8 Hz, Ar), 7.62 (d, 2H, *J* = 15.6 Hz, CH=CH). ^{13}C-NMR (101 MHz, $CDCl_3$): δ 70.89 (2C), 114.50, 115.01 (d, 4C, *J* = 27.3 Hz), 115.72 (4C), 122.97, 128.89, 129.42 (4C), 129.47 (2C), 129.71 (d, 4C, *J* = 8.1 Hz), 131.94 (d, 2C, *J* = 4.0 Hz), 140.82 (2C), 159.67 (2C), 162.49 (d, 2C, *J* = 265.6 Hz), 183.76 (2C). ESI-MS (*m/z*): 547 (M + Na).

1*E*,4*Z*,6*E*-1,7-bis-4-(3-fluorobenzyloxyphenyl)-5-hydroxyhepta-1,4,6-trien-3-one (12).

Reaction of pentane-2,4-dione (0.50 g, 5.00 mmol), B_2O_3 (0.35 g, 5.00 mmol), and 4-(3-fluorobenzyloxybenzaldehyde **20** (2.07 g, 9.00 mmol) gave a crude product, that was purified by flash chromatography (PE / EtOAc, 9:1), 35 % yield, yellow solid, mp 160-162 °C. ^{1}H-NMR (400 MHz, $CDCl_3$): δ 5.10 (s, 4H, OCH_2), 5.78 (s, 1H, keto-enol-CH), 6.51 (d, 2H, *J* = 15.6 Hz, CH=CH), 6.98 (d, 4H, *J* = 8.8 Hz, Ar), 7.01-7.05 (m, 2H, Ar), 7.16-7.18 (m, 2H, Ar), 7.20-7.22 (m, 2H, Ar), 7.35-7.37 (m, 2H, Ar), 7.51 (d, 4H, *J* = 8.8 Hz, Ar), 7.62 (d, 2H, *J* = 15.6 Hz, CH=CH). ^{13}C-NMR (101 MHz, $CDCl_3$): δ 72.62 (2C), 114.16 (d, 2C, *J* = 28.3 Hz), 115.07 (d, 2C, *J* = 26.3 Hz), 115.27 (5C), 123.31, 123.63 (d, 2C, *J* = 4.0 Hz), 127.81 (4C), 128.99 (3C), 129.28 (d, 2C, *J* = 8.1 Hz), 140.80 (d, 2C, *J* = 6.9 Hz), 143.82 (2C), 160.59 (2C), 163.07 (d, 2C, J = 264.6 Hz), 183.67 (2C). ESI-MS (*m/z*): 547 (M + Na).

Williamson reaction: General Procedure for the Synthesis of 8-10, 13-16.

To a solution of phenol-derivative (1.00 mmol) in acetone (10.0 mL), anhydrous K_2CO_3 (2.2 molar equiv) and the appropriate alkyl or aryl halide (2.2 molar equiv) were added. The reaction mixture was heated to 80 °C and reaction progress was monitored by TLC. Upon reaction completion, the mixture was hot filtered and the solvent was evaporated under reduced pressure. The two tautomers obtained were effectively isolated from the resulting crude mixture by column chromatography over silica gel and using a mixture of PE / EtOAc as eluent. The desired final

compounds were further purified by fractionated crystallization from DCM / PE. In particular, regarding the order of elution of the tautomeric mixtures, the β-diketo tautomer proved to elute first.

1*E*,4*Z*,6*E*-1,7-bis-4-benzyloxyphenyl-5-hydroxyhepta-1,4,6-trien-3-one (8) and 1*E*,6*E*-1,7-bis-4-benzyloxyphenylhepta-1,6-diene-3,5-dione (14). Reaction of **4** (0.50 g, 1.62 mmol), K_2CO_3 (0.49 g, 3.56 mmol), and benzyl bromide (0.47 mL, 3.56 mmol) gave a tautomeric mixture that was purified by flash chromatography (PE / EtOAc, 9:1). **8** (Rf: 0.12), experimental characterization matched with that of the same analogue obtained by the Pabon reaction (see above). **14** (Rf: 0.15), 32 % yield, dark-yellow powder, mp 145-147 °C. ^{1}H-NMR (400 MHz, $CDCl_3$): δ 3.96 (s, 2H, β-diketo-CH_2), 5.08 (s, 4H, OCH_2), 6.87 (d, 2H, *J* = 16.0 Hz, CH=CH), 6.94 (d, 4H, *J* = 8.4 Hz, Ar), 7.35-7.39 (m, 10H, Bz) 7.52 (d, 4H, *J* = 8.4 Hz, Ar), 7.73 (d, 2H, *J* = 16.0 Hz, CH=CH). ^{13}C-NMR (101 MHz, $CDCl_3$): δ 55.73, 70.44 (2C), 115.60 (4C), 122.27 (2C), 127.85 (4C), 128.40 (2C), 128.50 (2C), 129.20 (4C), 130.00 (4C), 136.91 (2C), 140.50 (2C), 160.80 (2C), 196.37 (2C). ESI-MS (*m/z*): 511 (M + Na).

1*E*,4*Z*,6*E*-1,7-bis-4-(2,4-difluorobenzyloxy)phenyl)-5-hydroxyhepta-1,4,6-trien-3-one (9) and 1*E*,6*E*-1,7-bis-4-(2,4-difluorobenzyloxyphenyl)hepta-1,6-diene-3,5-dione (15). Reaction of **4** (0.50 g, 1.60 mmol) and 2,4-difluorobenzyl bromide (0.48 mL, 3.52 mmol) gave a crude that was purified by flash chromatography (PE / EtOAc, 9.5:0.5). **9** (Rf: 0.13), yellow powder, 32 % yield, 174-176 °C. ^{1}H-NMR (400 MHz, $CDCl_3$): δ 5.12 (s, 4H, OCH_2), 5.79 (s, 1H, keto-enol-CH), 6.51 (d, 2H, *J* = 16.0 Hz, CH=CH), 6.84-6.95 (m, 4H, Ar), 6.99 (d, 4H, *J* = 8.4 Hz, Ar), 7.46-7.48 (m, 2H, Ar), 7.52 (d, 4H, *J* = 8.4 Hz, Ar), 7.61 (d, 2H, *J* = 16.0 Hz, CH=CH). ^{13}C-NMR (101 MHz, $CDCl_3$): δ 63.50 (2C), 104.00 (t, 2C, *J* = 25.6 Hz), 111.63 (dd, 2C, *J* = 21.4 and 3.8 Hz), 114.98 (4C), 115.17, 119.13 (dd, 2C, *J* = 14.6 and 4.0 Hz), 123.31, 128.48 (4C), 128.50 (2C), 130.52, 130.85 (dd, 2C, *J* = 9.8 and 5.3 Hz), 140.81 (2C), 160.74 (dd, 2C, *J* = 238.4 and 12.0 Hz), 163.23 (dd, 2C, *J* = 237.9 and 12.0 Hz), 163.39 (2C), 183.65 (2C). ESI-MS (*m/z*): 583 (M + Na). **15** (Rf: 0.16), yellow powder, 28 % yield, 153-155 °C. ^{1}H-NMR (400 MHz, $CDCl_3$): δ 3.98 (s, 2H, β-

diketo-CH_2), 5.11 (s, 4H, OCH_2), 6.82 (d, 2H, *J* = 15.6 Hz, CH=CH), 6.88-6.92 (m, 4H, Ar), 6.96 (d, 4H, *J* = 8.4 Hz, Ar), 7.10-7.12 (m, 2H, Ar), 7.46 (d, 4H, *J* = 8.8 Hz, Ar), 7.75 (d, 2H, *J* = 15.6 Hz, CH=CH). ^{13}C-NMR (101 MHz, $CDCl_3$): δ 55.43, 63.49 (2C), 104.04 (t, 2C, *J* = 25.7 Hz), 111.62 (dd, 2C, *J* = 21.9 and 4.0 Hz), 116.37 (4C), 119.20 (dd, 2C, *J* = 15.1 and 4.5 Hz), 126.43 (2C), 128.59 (4C), 129.02 (2C), 130.90 (dd, 2C, *J* = 10.6 and 5.4 Hz), 143.07 (2C), 160.60 (dd, 2C, *J* = 238.7 and 12.2 Hz), 160.80 (2C), 163.03 (dd, 2C, *J* = 238.6 and 12.2 Hz), 196.30 (2C). ESI-MS (*m/z*): 583 (M + Na).

1*E*,4*Z*,6*E*-1,7-bis-4-(3,5-difluorobenzyloxyphenyl)-5-hydroxyhepta-1,4,6-trien-3-one (10) and 1*E*,6*E*-1,7-bis-4-(3,5-difluorobenzyloxyphenyl)hepta-1,6-diene-3,5-dione (16). Reaction of **4** (0.50 g, 1.60 mmol) and 3,5-difluorobenzyl bromide (0.48 mL, 3.52 mmol) gave a crude that was purified by flash chromatography (PE / EtOAc, 9.5:0.5). **10** (Rf: 0.11), 60 %, yield, mp 174-176 °C. ^{1}H-NMR (400 MHz, $CDCl_3$): δ 5.09 (s, 4H, OCH_2), 5.80 (s, 1H, keto-enol-CH), 6.52 (d, 2H, *J* = 15.6 Hz, CH=CH), 6.56-6.67 (m, 2H, Ar), 6.73-6.81 (m, 2H, Ar), 6.93-6.99 (m, 2H, Ar), 6.97 (d, 4H, *J* = 8.8 Hz, Ar), 7.52 (d, 4H, *J* = 8.8 Hz, Ar), 7.63 (d, 2H, *J* = 15.6 Hz, CH=CH). ^{13}C-NMR (101 MHz, $CDCl_3$) δ 71.64 (2C), 102.80 (t, 2C, *J* = 27.7 Hz), 112.18 (dd, 4C, *J* = 27.3 and 4.0 Hz), 114.99, 115.14 (4C), 122.98, 128.87 (4C), 129.05, 130.10 (2C), 141.60 (t, 2C, *J* = 7.2 Hz), 143.81 (2C), 159.97 (2C), 164.26 (dd, 4C, *J* = 261.8 and 6.9 Hz), 183.50 (2C) ESI-MS (*m/z*): 583 (M + Na). **16** (Rf: 0.13) yellow powder, 28 % yield, mp 152-154 °C. ^{1}H-NMR (400 MHz, $CDCl_3$): δ 3.94 (s, 2H, β-diketo-CH_2), 5.07 (s, 4H, OCH_2), 6.60-6.72 (m, 2H, Ar), 6.75 (d, 2H, *J* = 15.2 Hz, CH=CH), 6.79-6.84 (m, 2H, Ar), 6.93 (d, 4H, *J* = 8.4 Hz, Ar), 6.93-6.98 (m, 2H, Ar), 7.43 (d, 4H, *J* = 8.8 Hz, Ar), 7.75 (d, 2H, *J* = 15.2 Hz, CH=CH). ^{13}C-NMR (101 MHz, $CDCl_3$) δ 55.84, 71.73 (2C), 102.98 (t, 2C, *J* = 27.7 Hz), 112.20 (dd, 4C, *J* = 27.0 and 4.0 Hz), 115.30 (4C), 127.13 (2C), 129.48 (4C), 129.50 (2C), 140.57 (t, 2C, *J* = 6.8 Hz), 142.41 (2C), 160.59 (2C), 164.20 (dd, 4C, *J* = 261.3 and 6.4 Hz) 195.06 (2C). ESI-MS (*m/z*): 583 (M + Na).

1*E*,6*E*-1,7-bis-4-methoxyphenylhepta-1,6-diene-3,5-dione (13). Reaction of **4** (0.15 g, 0.49 mmol), K_2CO_3 (0.14 g, 0.98 mmol), and iodomethane (0.06 mL, 0.98 mmol) gave the crude that was purified by flash chromatography (PE / EtOAc, 9.5:0.5) from which **13** was obtained as predominant component, orange-yellow powder, 44 % yield, mp 103-105 °C. ^{1}H-NMR (400 MHz, $CDCl_3$) δ 3.48 (s, 2H, β-diketo-CH_2), 3.86 (s, 6H, OCH_3), 6.93 (d, 4H, *J* = 8.8 Hz, Ar), 7.01 (d, 2H, *J* = 14.8 Hz, CH=CH), 7.55 (d, 4H, *J* = 6.8 Hz, Ar), 7.72 (d, 2H, *J* = 14.8 Hz, CH=CH). ^{13}C-NMR (101 MHz, $CDCl_3$) δ 55.38 (2C), 55.43, 114.37 (4C), 121.80 (2C), 128.24 (2C), 129.75 (4C), 141.20 (2C), 161.37 (2C), 196.57 (2C). ESI-MS (*m/z*): 359 (M + Na).

4-(4-fluorobenzyloxy)benzaldehyde (**19)**. Reaction of 4-hydroxybenzaldehyde (1.24 g, 10.00 mmol) and 4-fluorobenzylbromide (1.49 mL, 12.00 mmol) gave a crude that was purified by flash chromatography (PE / EtOAc, 9.5:0.5), white solid, 88 % yield, mp 190-192 °C. ^{1}H-NMR (400 MHz, $CDCl_3$): δ 5.08 (s, 2H, OCH_2), 6.99-7.00 (m, 2H, Ar), 7.02 (d, 2H, *J* = 8.8 Hz, Ar), 7.10-7.14 (m, 2H, Ar), 7.82 (d, 2H, J = 8.8 Hz, Ar), 9.80 (s, 1H, CHO).

4-(3-fluorobenzyloxy)benzaldehyde (**20).** Reaction of 4-hydroxybenzaldehyde (1.24 g, 10.00 mmol) and 3-fluorobenzylbromide (1.49 mL, 12.00 mmol) gave a crude that was purified by flash chromatography (PE / EtOAc, 9.5:0.5), white solid, 85 % yield, mp 183-185 °C. ^{1}H-NMR (400 MHz, $CDCl_3$): δ 5.10 (s, 2H, OCH_2), 6.95 (d, 2H, *J* = 8.8 Hz, Ar), 6.93-6.99 (m, 1H, Ar), 7.00-7.07 (m, 2H, Ar), 7.23-7.31 (m, 1H, Ar), 7.84 (d, 2H, *J* = 8.8 Hz, Ar), 9.80 (s, 1H, CHO).

Chemical Stability Studies.

The tested derivative were dissolved in DMSO (0.50 mg / mL) and the pH of the solution was adjusted to 7.4 and 9.2 using 50 mM phosphate and 50 mM borate buffer, respectively. The obtained solutions were then maintained at room temperature and at 70°C (oven) for three days and analyzed by RP-HPLC under the following conditions: the stationary phase was a phenyl-hexyl column (Xselect CSH by Waters) 4.6 x 150 mm (particle size 3.5 µm); the mobile phase was a

mixture of ACN-0.1 % formic acid, 70-30 (v / v) at the flow rate of 1 mL / min. The detection wavelength was 254 nm.

BACE-1 inhibition.

FRET inhibition studies were performed using the following procedures: 5 μL of test compound (or DMSO) were pre-incubated with 175 μL of BACE-1 (17.2 nM, final concentration) in 20 mM sodium acetate pH 4.5 containing CHAPS (0.1 % w / v) for 1 hour at room temperature. M-2420 (3 μM, final concentration) was then added and left to react for 15 min at 37 °C. The fluorescence signal was read at λ_{em} = 405 nm (λ_{exc} = 320 nm). DMSO concentration in the final mixture was maintained below 5 % (v / v) to guarantee no significant loss of enzyme activity. Fluorescence intensities with and without inhibitors were registered and compared. The percent inhibition due to the presence of test compounds was calculated. The background signal was measured in control wells containing all the reagents, except hrBACE-1, and subtracted. The % inhibition due to the presence of test compound was calculated by the following expression: $100-(IF_i / IF_o \times 100)$ where IF_i and IF_o are the fluorescence intensities obtained for hrBACE-1 in the presence and in the absence of inhibitor, respectively.[41] The linear regression parameters were determined and the IC_{50} interpolated (GraphPad Prism 4.0, GraphPad Software Inc.). To demonstrate inhibition of BACE-1 activity a peptido-mimetic inhibitor (β-secretase inhibitor IV, Calbiochem) was serially diluted into the reactions' wells (IC_{50} = 20 nM).

Inhibition of GSK-3β.

Human recombinant GSK-3β was purchased from Millipore (Millipore Iberica S.A.U.). The prephosphorylated polypeptide substrate was purchased from Millipore (Millipore Iberica SAU). Kinase-Glo Luminescent Kinase Assay was obtained from Promega (Promega Biotech Iberica, SL). ATP and all other reagents were from Sigma-Aldrich (St. Louis, MO). Assay buffer contained 50 mM HEPES (pH = 7.5), 1 mM EDTA, 1 mM EGTA, and 15 mM magnesium acetate. The method of Baki et al.[44] was followed to analyze the inhibition of GSK-3β. Kinase-Glo assays were

performed in assay buffer using white 96-well plates. In a typical assay, 10 μL (10 μM) of tested compound (dissolved in dimethyl sulfoxide (DMSO) at 1 mM concentration and diluted in advance in assay buffer to the desired concentration) and 10 μL (20 ng) of enzyme were added to each well followed by 20 μL of assay buffer containing 25 μM substrate and 1 μM ATP. The final DMSO concentration in the reaction mixture did not exceed 1 %. After a 30 min incubation at 30 °C, the enzymatic reaction was stopped with 40 μL of Kinase-Glo reagent. Glow-type luminescence was recorded after 10 min using a Fluoroskan Ascent multimode reader. The activity is proportional to the difference of the total and consumed ATP. The inhibitory activities were calculated on the basis of maximal kinase and luciferase activities measured in the absence of inhibitor and in the presence of reference compound inhibitor (SB415826,[63] supplier, IC50 = 54 nM) at total inhibition concentration, respectively. The linear regression parameters were determined and the IC_{50} extrapolated (GraphPad Prism 4.0, GraphPad Software Inc.).

Docking studies on GSK-3β.

A SCARE docking procedure was applied to generate the bound pose of curcumin at the binding site of GSK-3β (PDBid:1Q5K). This specific crystal structure was selected in light of the suitable results obtained in previous exploratory docking studies.[64] The docking engine used was the Biased Probability Monte Carlo (BPMC) stochastic optimizer as implemented in ICM.[65] The binding site was represented by pre-calculated 0.5 Å spacing potential grid maps, representing van der Waals potentials for hydrogens and heavy atoms, electrostatics, hydrophobicity, and hydrogen bonding, respectively. The van der Waals interactions were described by a smoother form of the Lennard-Jones potential, capping the repulsive contribution to 4 kcal / mol. The binding energy was assessed with the ICM empirical scoring function.[66] The SCARE docking procedure was thoroughly described by Bottegoni at al.[67] and it is here only briefly summarized. Multiple variants of the binding pocket were generated introducing ‘gaps’ in the structure, namely recalculating the potential grid maps describing the binding site excluding each time the side chains of a pair of

proximal residues. Thirty-two gapped variants were generated and stored in a 4D grid. A multiple receptor conformation docking was carried out.[67] Thoroughness was set equal to 20. Thirty initial bound poses (seeds) of the ligand were generated and retained. The original complement of side chains was restored and each seed underwent a refinement procedure according to the original SCARE protocol.[67] After refinement, the best scoring curcumin-optimized binding pocket complex was selected and used as template in a template docking step to generate the bound pose of **5-8**.

Docking studies on BACE-1.

The receptor structure was selected performing an APF superimposition[68] between curcumin and the co-crystallized ligands of the seven BACE-1 complexes previously studied by Kacker et al.[69] The hydroxyethylamine-based inhibitor returned the best superimposition and its cognate receptor conformation was selected for docking (PDBid:1W51). Initially, a gapped model of the receptor was generated excluding from the complement of maps the residues of the flap (residues 65:77). The catalytic dyad was assigned the 32i protonation state.[69] Curcumin was docked at the binding site of the gapped model. After docking, the flap conformation was optimized by means of BPMC performed on the ligand receptor complex.[70] In the loopmodel macro, default parameters were adopted. The bound pose of curcumin at the optimized pocket was used as template to guide the docking of **5-8**.[71]

Cell culture.

The T67 human glioma cell line was derived by Lauro et al. from a World Health Organization (WHO) Grade III gemistocytic astrocytoma. T67 cells were cultured in Dulbecco's modified Eagle's medium (DMEM) supplemented with 10 % fetal bovine serum (FBS), 100 UI / mL penicillin, 100 µg / mL streptomycin in a 5 % CO_2 atmosphere at 37 °C, with saturating humidity.

Determination of antioxidant activity in T67 cells.

To evaluate the antioxidant activity of the compounds, T67 cells were seeded in 24-well plates at 1 x 10^5 cells / well. After 24 hours, the cells were washed with PBS and treated for 24 hours with

the compounds at 10 µM concentration. The antioxidant activity of the compounds was evaluated after 30 minutes of incubation with 10 µM fluorescent probe (2',7'-dichlorofluorescein diacetate, DCFH-DA) in DMEM, by measuring the intracellular ROS formation evoked by 30 minutes exposure of T67 cells to 100 µM tert-butyl hydroperoxide (TBH) in PBS. The fluorescence increase of the cells from each well was measured (λexc = 485 nm; λem = 535 nm) with a spectrofluorometer (Wallac Victor multilabel S9 counter, Perkin-Elmer Inc., Boston, MA). Data are reported as the mean ± standard deviation of at least three independent experiments.

Determination of cell viability (Cytotoxicity Assays)

Cytotoxicity of compounds was estimated using an MTT assay. T67 cells were seeded with complete DMEM in 24-well plates and cultured overnight. Cells were washed with PBS and incubated for 24 hours at 37 °C in humidified atmosphere, 5 % CO_2, with compounds at different concentrations dissolved in DMEM. After this time, cells were carefully washed with PBS and incubated for 3 h with 500 µM thiazolyl blue tetrazolium bromide (MTT) dissolved in DMEM. Then, cells were washed with PBS and lysed with 200 µL of dimethyl sulfoxide. The absorbance of each well was measured at 595 nm using a microplate reader (Victor2 1420 multilabel counter).

Preparation of cell homogenate

T67 cells were treated for 24 hours with [10 µM] of compounds and [2.5 µM] of 4-methylsulfinylbutyl isothiocyanate (sulforaphane) as positive control. After this time, cells were collected and resuspended in ice-cold 50 mM potassium phosphate buffer, pH 7.4, containing 2 mM EDTA and 0.1 % Triton X-100.

Assay for NQO1 induction.

Cellular NQO1 activity was measured according to the procedures described previously.[72] Briefly, the reaction mix contained 50 mM Tris–HCl, pH 7.5, 0.08 % Triton X-100, 0.25 mM NADPH, and 80 µM of 2,6-dichloroindophenol (DCIP) in the presence or absence of 10 µM dicumarol. To an assay cuvette, 0.980 mL of the reaction mix was added and the reaction was

started by adding 20 µL of cell homogenate and the reduction of DCIP was monitored at 600 nm, 30 °C for 3 min. The dicumarol-inhibitable NQO1 activity was calculated using the extinction coefficient of 21.0 mM^{-1} cm^{-1} and expressed as nmol of DCIP reduced per min / mg of cellular protein determined by Lowry method.[72]

Determination of the Chemical Stability

Vehicle (DMSO), **5** and **13** (0.5 mg / mL) at pH 7.4 and 9.2 (adjusted with aqueous buffers) were incubated for three days at 70 °C (oven).

Table 1. Inhibition of BACE-1 and GSK-3β enzymatic activities by the curcumin-based analogues as keto-enol tautomer (**2-12**) and reference compound curcumin (**1b**).

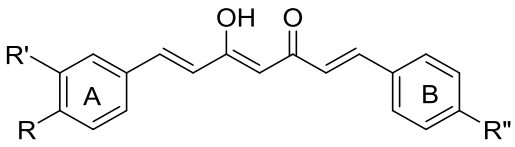

				IC_{50} (μM)[a] ± SEM	
comp	**R**	**R'**	**R"**	**BACE-1**	**GSK-3β**
2	OH	OCH_3	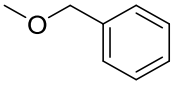	0.97 ± 0.43	0.90 ± 0.38
3	OH	OCH_3	CH_3	0.14 ± 0.03	2.09 ± 0.51
4	OH	H	OH	2.54 ± 0.02	8.39 ± 1.59
5	OCH_3	H	OCH_3	1.65 ± 0.01 17 ± 3[c]	0.53 ± 0.27
6	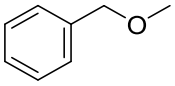	H	OCH_3	2.28 ± 0.64	2.78 ± 0.44
7	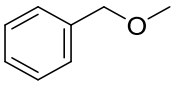	H	OH	2.69 ± 1.01	2.01 ± 0.71
8	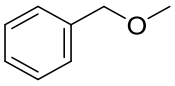	H	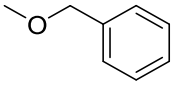	0.04 ± 0.01	2.49 ± 0.82
9	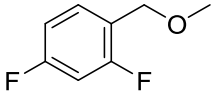	H	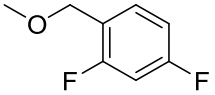	0.40 ± 0.06	9.63 ± 0.21
10	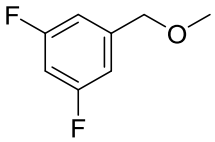	H	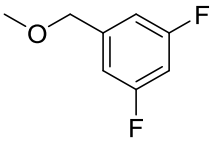	0.39 ± 0.34	8.30 ± 0.54
11	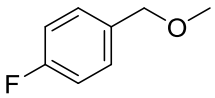	H	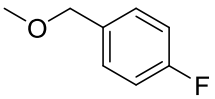	1.04 ± 0.34	12.81 ± 0.14
12	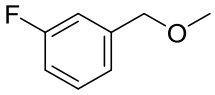	H	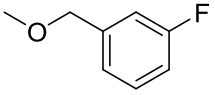	1.08 ± 0.66	16.99 ± 2.68

Cur	n.i.[b]	17.95 ± 1.03
cumin	343 ± 45[c]	

[a]Values are mean ± S.D. of two independent measurements, each performed in triplicate. SEM = standard error of the mean. [b]n.i.: not inhibiting up to 3 μM. [c] Data taken from reference [39].

Table 2. Inhibition of BACE-1 and GSK-3β enzymatic activities by the curcumin-based analogues as β-diketo tautomer (**13-16**).

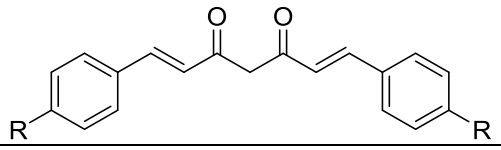

		IC_{50} (μM)[a] ± SEM	
comp	**R**	**BACE-1**	**GSK-3β**
13	OCH_3	> 5	15.30 ± 3.64
14	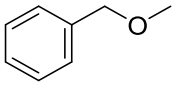	6.04 ± 0.57	5.56 ± 0.01
15	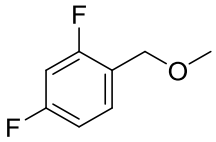	1.00 ± 0.35	9.06 ± 2.07
16	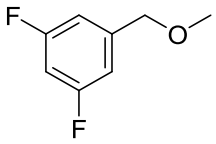	0.73 ± 0.24	9.66 ± 1.02

[a] Values are mean ± S.D. of two independent measurements, each performed in triplicate. SEM = standard error of the mean.

Table 3. Permeability (*Pe* 10^{-6} cm s^{-1}) in the PAMPA-BBB assay for the selected compounds (**2-8**) with their predictive penetration in the CNS.

Comp[a]	***Pe*** **(10^{-6} cm s^{-1})**[b]	**Prediction**
2	7.7 ± 1.8	CNS +
3	8.2 ± 1.3	CNS +
5	2.8 ± 0.3	CNS + / CNS -
6	7.0 ± 0.7	CNS +
7	7.8 ± 0.2	CNS +

8	3.6 ± 0.1	CNS + / CNS-
curcumin (1b)	2.5 ± 0.1	CNS + / CNS -

[a]PBS:EtOH (70:30) was used as solvent. [b]Data are the mean ± SD of 2 independent experiments.

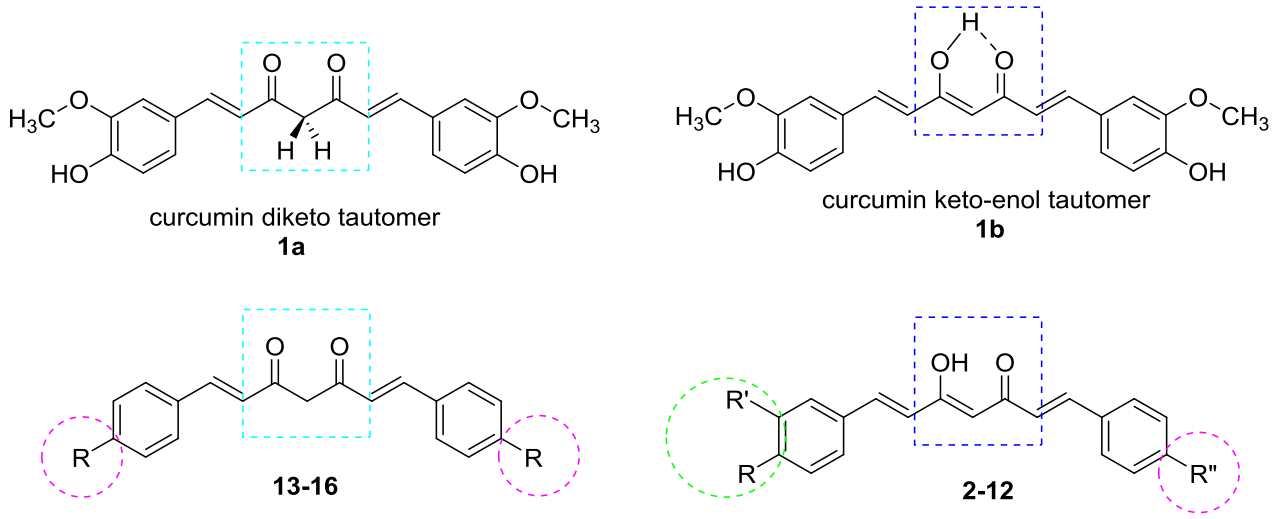

Figure 1. Design Strategy toward the synthetized curcumin-based analogues (2-16). Structure of the tautomeric forms of curcumin (β-diketo tautomer **1a** and keto-enol tautomer **1b**) and general formula of the synthetized curcumin-based analogues (**2-12** and **13-16**). For structures see tables 1 and 2.

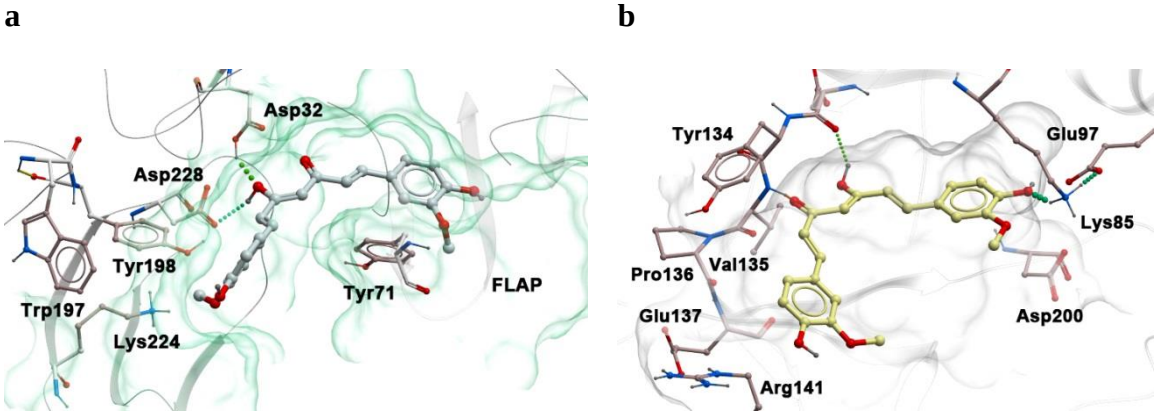

Figure 2. Curcumin **1b** docked into the catalytic region of a) BACE-1and b) GSK-3β.

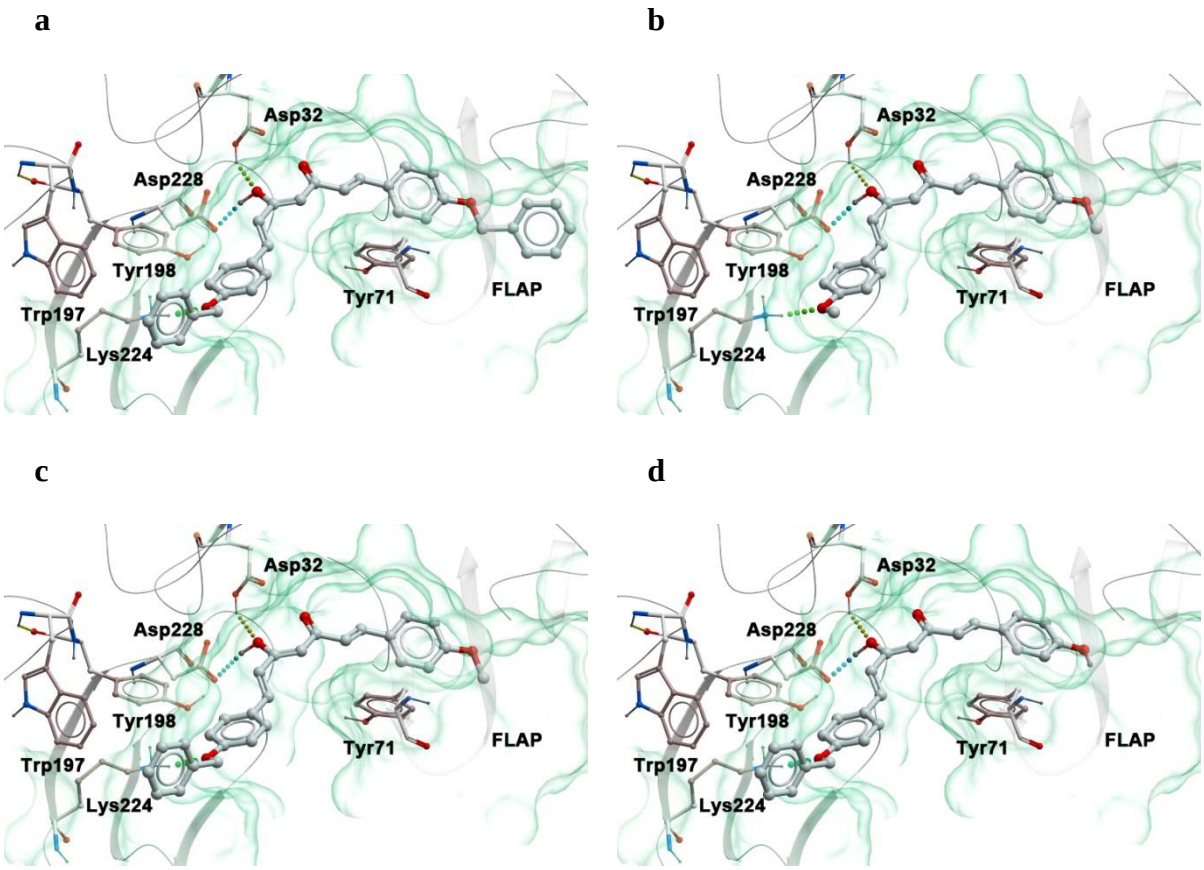

Figure 3. The predicted bound conformation of a) **8**, b) **5**, c) **6**, d) **7** at the binding site of BACE-1. The ligand is reported in light grey x-sticks. The key residues of the binding site are reported in x-sticks and labeled explicitly. A transparent green mesh describes the boundaries of the binding site.

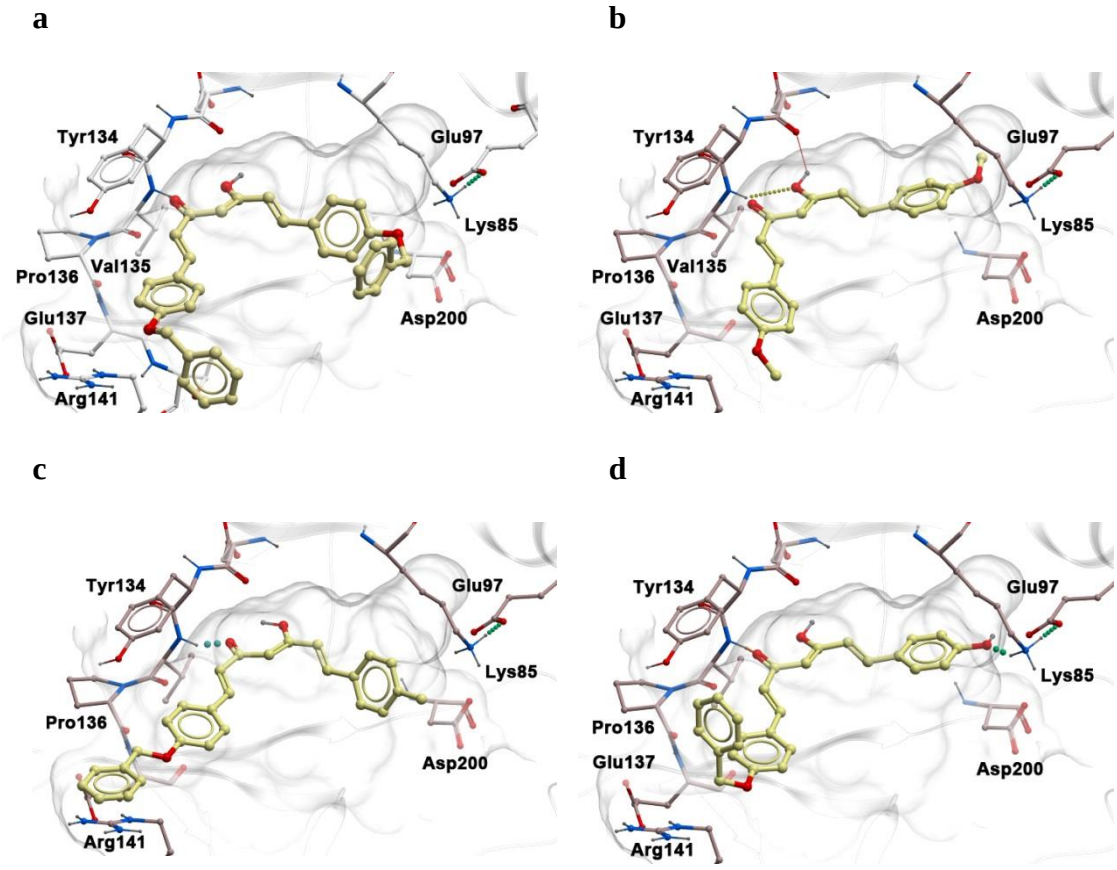

Figure 4. The predicted bound conformation of a) **8**, b) **5**, c) **6**, d) **7** at the binding site of GSK-3β. The ligand is reported in yellow x-sticks. The key residues of the binding site are reported in x-sticks and labeled explicitly. A transparent white mesh describes the boundaries of the binding site. For clarity, the glycine-rich loop is not reported.

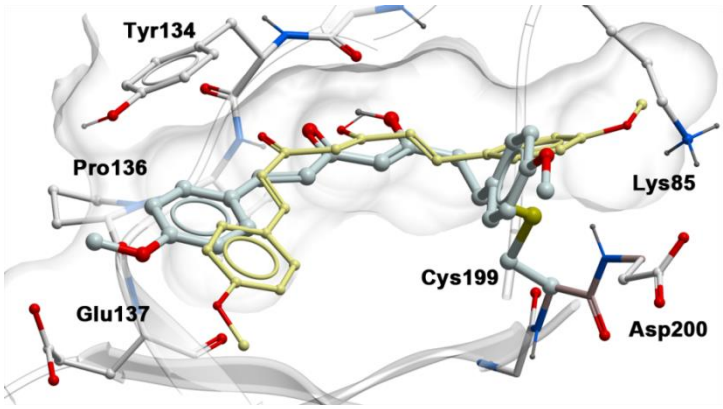

Figure 5. The predicted covalent bound conformation of **5** at the binding site of GSK-3β. A covalent docking was accomplished in which a thia-Michael reaction occurred by nucleophilic attack of GSK-3β Cys199 residue on the reactive α,β-unsaturated carbonyl function of **5**. The conformation then adopted by **5** stabilizes even further the interactions within the hinge region of GSK-3β. The ligand is reported in yellow (reference binding mode) and grey x-sticks (from covalent docking). The key residues of the binding site are reported in white-sticks and labeled explicitly. A transparent white mesh describes the boundaries of the binding site. For clarity, the glycine-rich loop is not reported.

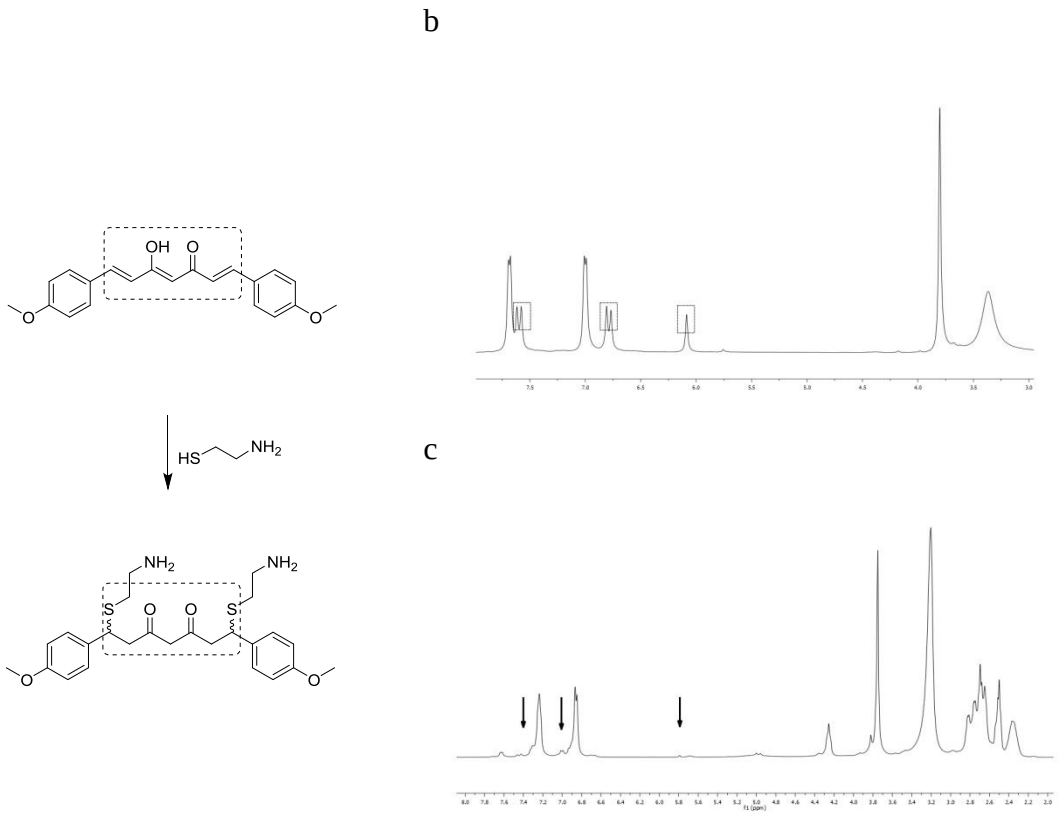

Figure 6. Thiol trapping assay. a) Reaction of **5** with cysteamine. b) ^{1}H-NMR spectrum of **5** in *d*6-DMSO. In the squares the signals of the α,γ-unsaturated-keto-enol system are indicated. c) ^{1}H-NMR spectrum of **5**-positive assay, in *d*6-DMSO, with a 1:2 stoichiometric ratio of 5 / cysteamine. The arrows indicate the disappearance of the above-mentioned signals.

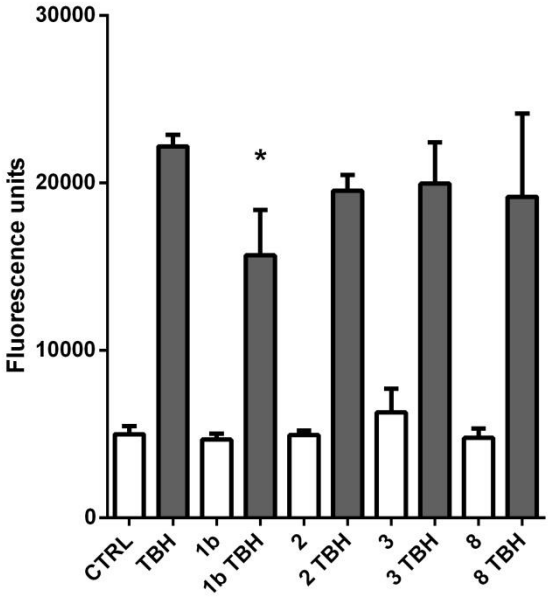

Figure 7. Effect of **2**, **3**, and **8** and on ROS formation in T67 cells, in comparison with curcumin **1b** as the reference. The antioxidant potential was estimated as ROS scavenging ability. The compounds, at the fixed concentration of 10 μM, were exposed to 100 μM TBH and then incubated with 10 μM of the fluorescent probe DCFH-DA; the increase in fluorescence was related to the intracellular ROS formation. Data are reported as the mean ± standard deviation of at least three independent experiments.

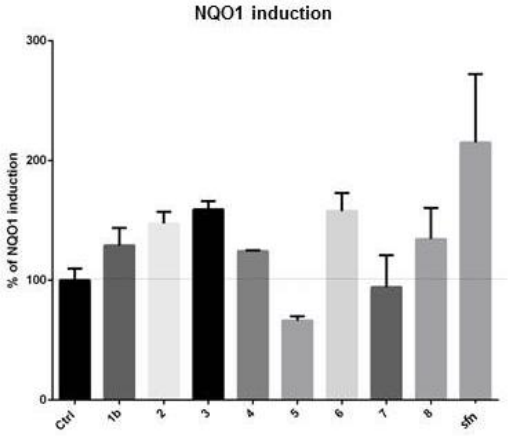

Figure 8. NQO1 induction potential of curcumin **1b** and analogues **2-8**. Compounds, tested at 10 μM concentration, were evaluated for their dicumarol-inhibitable NQO1 activity on T67 cells, after treatment with 2.5 μM of sulforaphane (**sfn**), a potent NQO1 inducer.

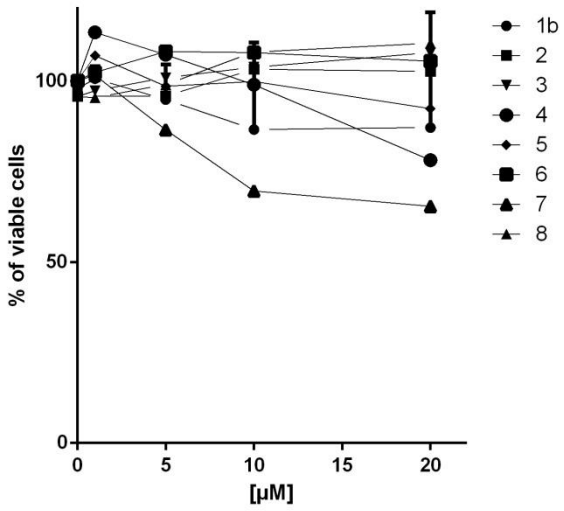

Figure 9. Cytotoxicity of compounds 2-8. The toxic effect in T67 cell lines, was estimated by MTT assay after 24 h treatment, using curcumin (**1b**) as the reference compound. Results are expressed as percentage of controls and are the mean ± SEM of four different experiments run at least in quadruplicate.

Scheme1.[a] General synthetic method for mono-aryl curcumin intermediates (**17**, **18**) and asymmetric curcumin-based analogues (**2**, **3**, **6**, **7**)

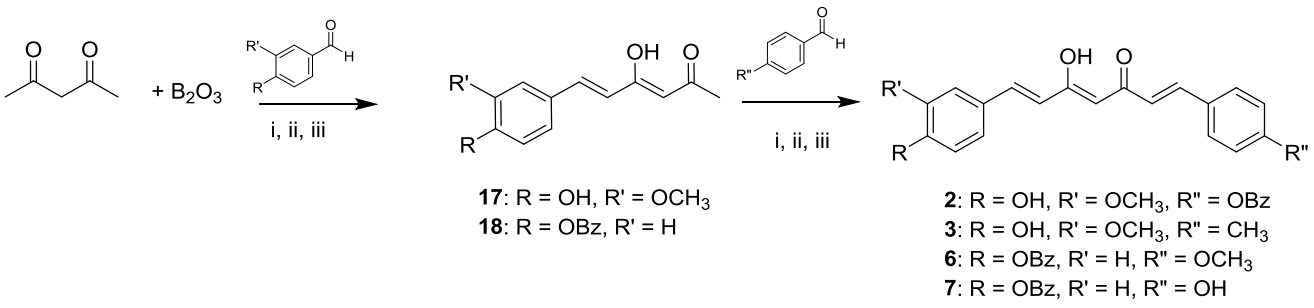

[a]**Reagents and conditions:** i) B(*n*-BuO)$_3$; ii) n-BuNH_2, 80 °C; iii) HCl, 80 °C.

Scheme 2.[a] General synthetic method for symmetric curcumin-based analogues **4**, **5**, **8**, **11**, and **12**.

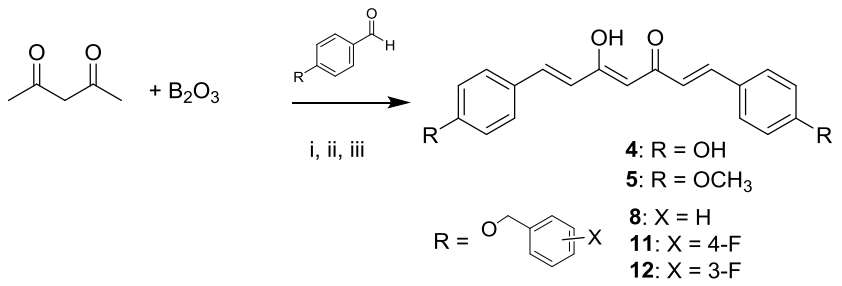

[a]**Reagents and conditions:** i) B(*n*-BuO)$_3$; ii) n-BuNH$_2$, 80 °C; iii) HCl, 80 °C.

Scheme 3.[a] General synthetic method for diketo tautomer **13**, and tautomeric couples **8** and **14**, **9** and **15**, **10** and **16**.

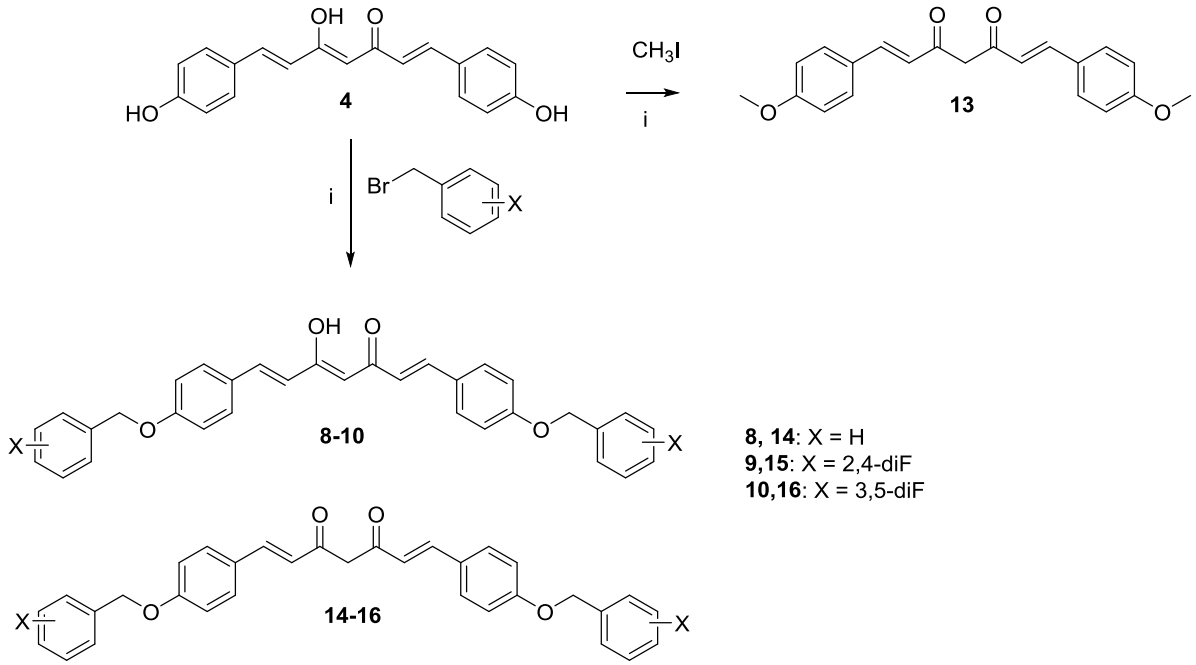

[a]**Reagents and conditions:** i) K_2CO_3, 80 °C.

Abbreviations

AD, Alzheimer's disease; BACE-1, β-secretase; GSK3-β, glycogen synthase kinase-3β; Aβ, amyloid β; SP, senile plaques; NFT, neurofibrillary tangles; APP, amyloid β protein precursor; NQO1, NAD(P)H:quinone oxidoreductase; CNS, central nervous system; ROS, reactive oxygen species; BBB, blood brain barrier; FRET, fluorescence resonance energy transfer; ADME,

Absorption, Distribution, Metabolism, Excretion; PAMPA, Parallel Artificial Membrane Permeability Assay; TBH, *tert*-butyl hydroperoxide.

Associated Content

Supporting Information Available: PAMPA-BBB assay for commercial drugs (Table S1), Linear correlation of PAMPA-BBB assay (Figure S1), Elemental analysis of synthesized compounds **2-16 (**Table S2). This material is available free of charge via the Internet at http://pubs.acs.org.

Author Information

Corresponding Author

F. Belluti: phone, +39-051-2099732; fax, +39-051-2099734; E-mail, federica.belluti@unibo.it.

Acknowledgments

This work was financially supported by a PRIN (20103W4779) Project Grant from MIUR, Italy.

The authors thank Prof. Roberto Gotti for performing the stability studies.

References

(1) Dulsat, C., A report from the 65th Annual Meeting of the American Academy of Neurology (March 16-23, 2013, San Diego, California, USA). *Drugs Today (Barc)* **2013,** *49* (5), 341-345.

(2) Cummings, J. L., Treatment of Alzheimer's disease: current and future therapeutic approaches. *Rev. Neurol. Dis.* **2004,** *1*, 60-69.

(3) Lazarov, O.; Marr, R. A., Neurogenesis and Alzheimer's disease: at the crossroads. *Exp. Neurol.* **2010,** *223*, 267-281.

(4) Marx, J., A New Take on Tau. *Science* **2007,** *316*, 1416-1417.

(5) Walsh, D. M.; Selkoe, D. J., Deciphering the molecular basis of memory failure in Alzheimer's disease. *Neuron* **2004,** *44*, 181-193.

(6) Schneider, L. S.; Mangialasche, F.; Andreasen, N.; Feldman, H.; Giacobini, E.; Jones, R.; Mantua, V.; Mecocci, P.; Pani, L.; Winblad, B.; Kivipelto, M., Clinical trials and late-stage drug development for Alzheimer's disease: an appraisal from 1984 to 2014. *J. Intern. Med.* **2014,** *275*, 251-283.

(7) Golde, T. E.; Eckman, C. B.; Younkin, S. G., Biochemical detection of Abeta isoforms: implications for pathogenesis, diagnosis, and treatment of Alzheimer's disease. *Biochim. Biophys. Acta* **2000,** *1502*, 172-187.

(8) Golde, T. E., Alzheimer disease therapy: can the amyloid cascade be halted? *J. Clin. Invest.* **2003,** *111*, 11-8.

(9) Ghosh, A. K.; Gemma, S.; Tang, J., beta-secretase as a therapeutic target for Alzheimer's disease. *Neurotherapeutics* **2008,** *5*, 399-408.

(10) Ittner, L. M.; Götz, J., Amyloid-β and tau--a toxic pas de deux in Alzheimer's disease. *Nat. Rev. Neurosci.* **2011,** *12*, 65-72.

(11) Weingarten, M. D.; Lockwood, A. H.; Hwo, S. Y.; Kirschner, M. W., A protein factor essential for microtubule assembly. *Proc. Natl. Acad. Sci. U S A* **1975,** *72*, 1858-1862.

(12) Avila, J., Tau phosphorylation and aggregation in Alzheimer's disease pathology. *FEBS Lett.* **2006,** *580*, 2922-2927.

(13) Llorens-Martín, M.; Jurado, J.; Hernández, F.; Avila, J., GSK-3β, a pivotal kinase in Alzheimer disease. *Front. Mol. Neurosci.* **2014,** *7*, 46.

(14) Billingsley, M. L.; Kincaid, R. L., Regulated phosphorylation and dephosphorylation of tau protein: effects on microtubule interaction, intracellular trafficking and neurodegeneration. *Biochem. J.* **1997,** *323*, 577-591.

(15) Martinez, A.; Perez, D. I.; Gil, C., Lessons Learnt from Glycogen Synthase Kinase 3 Inhibitors Development for Alzheimer's Disease. *Curr. Top. Med. Chem.* **2013,** *13*, 1808-1819.

(16) Perez, D. I.; Conde, S.; Perez, C.; Gil, C.; Simon, D.; Wandosell, F.; Moreno, F. J.; Gelpi, J. L.; Luque, F. J.; Martinez, A., Thienylhalomethylketones: Irreversible glycogen synthase kinase 3 inhibitors as useful pharmacological tools. *Bioorg. Med. Chem.* **2009,** *17*, 6914-6925; Perez, D. I.; Palomo, V.; Perez, C.; Gil, C.; Dans, P. D.; Javier Luque, F.; Conde, S.; Martinez, A., Switching Reversibility to Irreversibility in Glycogen Synthase Kinase 3 Inhibitors: Clues for Specific Design of New Compounds. *J. Med. Chem.* **2011,** *54* (12), 4042-4056.

(17) Busciglio, J.; Lorenzo, A.; Yeh, J.; Yankner, B. A., beta-amyloid fibrils induce tau phosphorylation and loss of microtubule binding. *Neuron* **1995,** *14*, 879-888.

(18) Zheng, W. H.; Bastianetto, S.; Mennicken, F.; Ma, W.; Kar, S., Amyloid beta peptide induces tau phosphorylation and loss of cholinergic neurons in rat primary septal cultures. *Neurosci.* **2002,** *115*, 201-211.

(19) Golde, T. E., Disease modifying therapy for AD? *J. Neurochem.* **2006,** *99*, 689-707.

(20) Grill, J. D.; Cummings, J. L., Current therapeutic targets for the treatment of Alzheimer's disease. *Expert. Rev. Neurother.* **2010,** *10*, 711-728.

(21) Cavalli, A.; Bolognesi, M. L.; Minarini, A.; Rosini, M.; Tumiatti, V.; Recanatini, M.; Melchiorre, C., Multi-target-directed ligands to combat neurodegenerative diseases. *J. Med. Chem.* **2008,** *51*, 347-372.

(22) Viayna, E.; Sola, I.; Di Pietro, O.; Muñoz-Torrero, D., Human disease and drug pharmacology, complex as real life. *Curr. Med. Chem.* **2013,** *20*, 1623-1634.

(23) Zheng, H.; Fridkin, M.; Youdim, M., From single target to multitarget/network therapeutics in Alzheimer's therapy. *Pharmaceuticals (Basel, Switzerland)* **2014,** *7*, 113-135.

(24) Morphy, R.; Kay, C.; Rankovic, Z., From magic bullets to designed multiple ligands. *Drug. Discov. Today.* **2004,** *9*, 641-651.

(25) Prati, F.; De Simone, A.; Bisignano, P.; Armirotti, A.; Summa, M.; Pizzirani, D.; Scarpelli, R.; Perez, D. I.; Andrisano, V.; Perez-Castillo, A.; Monti, B.; Massenzio, F.; Polito, L.; Racchi, M.; Favia, A. D.; Bottegoni, G.; Martinez, A.; Bolognesi, M. L.; Cavalli, A., Multitarget drug discovery for Alzheimer's disease: triazinones as BACE-1 and GSK-3β inhibitors. *Angew. Chem. Int. Ed. Engl.* **2015,** *54*, 1578-1582.

(26) Belluti, F.; De Simone, A.; Tarozzi, A.; Bartolini, M.; Djemil, A.; Bisi, A.; Gobbi, S.; Montanari, S.; Cavalli, A.; Andrisano, V.; Bottegoni, G.; Rampa, A., Fluorinated benzophenone derivatives: balanced multipotent agents for Alzheimer's disease. *Eur. J. Med. Chem.* **2014,** *78*, 157-166.

(27) Rizzo, S.; Tarozzi, A.; Bartolini, M.; Da Costa, G.; Bisi, A.; Gobbi, S.; Belluti, F.; Ligresti, A.; Allara, M.; Monti, J. P.; Andrisano, V.; Di Marzo, V.; Hrelia, P.; Rampa, A., 2-Arylbenzofuran-based molecules as multipotent Alzheimer's disease modifying agents. *Eur. J. Med. Chem.* **2012,** *58*, 519-532.

(28) Newman, D. J.; Cragg, G. M.; Snader, K. M., Natural products as sources of new drugs over the period 1981-2002. *J. Nat. Prod.* **2003,** *66*, 1022-1037.

(29) Evans, B. E.; Rittle, K. E.; Bock, M. G.; DiPardo, R. M.; Freidinger, R. M.; Whitter, W. L.; Lundell, G. F.; Veber, D. F.; Anderson, P. S., Methods for drug discovery: development of potent, selective, orally effective cholecystokinin antagonists. *J. Med.Chem.* **1988,** *31*, 2235-2246.

(30) Aggarwal, B. B.; Sundaram, C.; Malani, N.; Ichikawa, H., Curcumin: the Indian solid gold. *Adv. Exp. Med. Biol.* **2007,** *595*, 1-75.

(31) Prasad, S.; Gupta, S. C.; Tyagi, A. K.; Aggarwal, B. B., Curcumin, a component of golden spice: from bedside to bench and back. *Biotechnol. Adv.* **2014,** *32*, 1053-1064.

(32) Anand, P.; Thomas, S. G.; Kunnumakkara, A. B.; Sundaram, C.; Harikumar, K. B.; Sung, B.; Tharakan, S. T.; Misra, K.; Priyadarsini, I. K.; Rajasekharan, K. N.; Aggarwal, B. B., Biological activities of curcumin and its analogues (Congeners) made by man and Mother Nature. *Biochem. Pharmacol.* **2008,** *76*, 1590-1611.

(33) Chin, D.; Huebbe, P.; Pallauf, K.; Rimbach, G., Neuroprotective Properties of Curcumin in Alzheimer's Disease - Merits and Limitations. *Curr. Med. Chem.* **2013,** *20*, 3955-3985.

(34) Esatbeyoglu, T.; Huebbe, P.; Ernst, I. M.; Chin, D.; Wagner, A. E.; Rimbach, G., Curcumin--from molecule to biological function. *Angew. Chem. Int. Ed. Engl.* **2012,** *51*, 5308-5332.

(35) Payton, F.; Sandusky, P.; Alworth, W. L., NMR study of the solution structure of curcumin. *J. Nat. Prod.* **2007,** *70*, 143-146.

(36) Benassi, R.; Ferrari, E.; Lazzari, S.; Spagnolo, F.; Saladini, M., Theoretical study on Curcumin: A comparison of calculated spectroscopic properties with NMR, UV-vis and IR experimental data. *J. Molec. Struct.* **2008,** *892*, 168-176.

(37) Amslinger, S., The tunable functionality of alpha,beta-unsaturated carbonyl compounds enables their differential application in biological systems. *ChemMedChem* **2010,** *5*, 351-6.

(38) Bustanji, Y.; Taha, M. O.; Almasri, I. M.; Al-Ghussein, M. A.; Mohammad, M. K.; Alkhatib, H. S., Inhibition of glycogen synthase kinase by curcumin: Investigation by simulated molecular docking and subsequent in vitro/in vivo evaluation. *J. Enzyme Inhib. Med. Chem.* **2009,** *24*, 771-778.

(39) Wang, X.; Kim, J. R.; Lee, S. B.; Kim, Y. J.; Jung, M. Y.; Kwon, H. W.; Ahn, Y. J., Effects of curcuminoids identified in rhizomes of Curcuma longa on BACE-1 inhibitory and behavioral activity and lifespan of Alzheimer's disease Drosophila models. *BMC Complement. Altern. Med.* **2014,** *14*, 88.

(40) Pabon, H. J., A synthesis of curcumin and related compounds. Recl. Trav. Chim. Pays-Bas: 1964; Vol. 83, pp 379-386.

(41) Mancini, F.; De Simone, A.; Andrisano, V., Beta-secretase as a target for Alzheimer's disease drug discovery: an overview of in vitro methods for characterization of inhibitors. *Anal. Bioanal. Chem.* **2011,** *400*, 1979-1996.

(42) Hagmann, W. K., The many roles for fluorine in medicinal chemistry. *J. Med. Chem.* **2008,** *51* (15), 4359-4369.

(43) Silvestri, R., Boom in the development of non-peptidic beta-secretase (BACE1) inhibitors for the treatment of Alzheimer's disease. *Med. Res. Rev.* **2009,** *29*, 295-338.

(44) Baki, A.; Bielik, A.; Molnár, L.; Szendrei, G.; Keserü, G. M., A high throughput luminescent assay for glycogen synthase kinase-3beta inhibitors. *Assay Drug. Dev. Technol.* **2007,** *5*, 75-83.

(45) Kacker, P.; Bottegoni, G.; Cavalli, A., Computational methods in the discovery and design of BACE-1 inhibitors. *Curr. Med. Chem.* **2012,** *19*, 6095-6111.

(46) Minassi, A.; Sánchez-Duffhues, G.; Collado, J. A.; Muñoz, E.; Appendino, G., Dissecting the pharmacophore of curcumin. Which structural element is critical for which action? *J. Nat. Prod.* **2013,** *76*, 1105-1112.

(47) Avonto, C.; Taglialatela-Scafati, O.; Pollastro, F.; Minassi, A.; Di Marzo, V.; De Petrocellis, L.; Appendino, G., An NMR spectroscopic method to identify and classify thiol-trapping agents: revival of Michael acceptors for drug discovery? *Angew. Chem. Int. Ed. Engl.* **2011,** *50*, 467-471.

(48) Wang, Y. J.; Pan, M. H.; Cheng, A. L.; Lin, L. I.; Ho, Y. S.; Hsieh, C. Y.; Lin, J. K., Stability of curcumin in buffer solutions and characterization of its degradation products. *J. Pharm. Biomed. Anal.* **1997,** *15*, 1867-1876.

(49) Dahmke, I. N.; Boettcher, S. P.; Groh, M.; Mahlknecht, U., Cooking enhances curcumin anti-cancerogenic activity through pyrolytic formation of "deketene curcumin". *Food Chem.* **2014,** *151*, 514-519.

(50) Cardoso, F. L.; Brites, D.; Brito, M. A., Looking at the blood-brain barrier: molecular anatomy and possible investigation approaches. *Brain Res. Rev.* **2010,** *64*, 328-363.

(51) van Asperen, J.; Mayer, U.; van Tellingen, O.; Beijnen, J. H., The functional role of P-glycoprotein in the blood-brain barrier. *J. Pharm. Sci.* **1997,** *86*, 881-884.

(52) Begum, A. N.; Jones, M. R.; Lim, G. P.; Morihara, T.; Kim, P.; Heath, D. D.; Rock, C. L.; Pruitt, M. A.; Yang, F.; Hudspeth, B.; Hu, S.; Faull, K. F.; Teter, B.; Cole, G. M.; Frautschy, S. A., Curcumin structure-function, bioavailability, and efficacy in models of neuroinflammation and Alzheimer's disease. *J. Pharmacol. Exp. Ther.* **2008,** *326*, 196-208.

(53) Di, L.; Kerns, E. H.; Fan, K.; McConnell, O. J.; Carter, G. T., High throughput artificial membrane permeability assay for blood-brain barrier. *Eur. J. Med. Chem.* **2003,** *38*, 223-232.

(54) Crivori, P.; Cruciani, G.; Carrupt, P. A.; Testa, B., Predicting blood-brain barrier permeation from three-dimensional molecular structure. *J. Med. Chem.* **2000,** *43*, 2204-2216.

(55) Zhu, X.; Su, B.; Wang, X.; Smith, M. A.; Perry, G., Causes of oxidative stress in Alzheimer disease. *Cell. Mol. Life Sci.* **2007,** *64*, 2202-2210.

(56) Siegel, D.; Gustafson, D. L.; Dehn, D. L.; Han, J. Y.; Boonchoong, P.; Berliner, L. J.; Ross, D., NAD(P)H:quinone oxidoreductase 1: role as a superoxide scavenger. *Mol. Pharmacol.* **2004,** *65*, 1238-1247.

(57) Torres-Lista, V.; Parrado-Fernández, C.; Alvarez-Montón, I.; Frontiñán-Rubio, J.; Durán-Prado, M.; Peinado, J. R.; Johansson, B.; Alcaín, F. J.; Giménez-Llort, L., Neophobia, NQO1 and SIRT1 as premorbid and prodromal indicators of AD in 3xTg-AD mice. *Behav. Brain. Res.* **2014,** *271*, 140-146.

(58) Tsvetkov, P.; Asher, G.; Reiss, V.; Shaul, Y.; Sachs, L.; Lotern, J., Inhibition of NAD(P)H : quinone oxidoreductase 1 activity and induction of p53 degradation by the natural phenolic compound curcumin. *Proceed. Nat. Acad. Sci. U. S. A.* **2005,** *102*, 5535-5540.

(59) Capurro, V.; Busquet, P.; Lopes, J. P.; Bertorelli, R.; Tarozzo, G.; Bolognesi, M. L.; Piomelli, D.; Reggiani, A.; Cavalli, A., Pharmacological characterization of memoquin, a multi-target compound for the treatment of Alzheimer's disease. *PLoS One* **2013,** *8*, e56870.

(60) Manson, M. M., Inhibition of survival signalling by dietary polyphenols and indole-3-carbinol. *Eur. J. Cancer.* **2005,** *41*, 1842-1853.

(61) Lin, L.; Shi, Q.; Nyarko, A. K.; Bastow, K. F.; Wu, C. C.; Su, C. Y.; Shih, C. C.; Lee, K. H., Antitumor agents. 250. Design and synthesis of new curcumin analogues as potential anti-prostate cancer agents. *J. Med. Chem.* **2006,** *49*, 3963-3972.

(62) Saladini, M.; Lazzari, S.; Pignedoli, F.; Rosa, R.; Spagnolo, F.; Ferrari, E., New synthetic glucosyl-curcuminoids, and their (1)H and (13)C NMR characterization, from Curcuma longa L. *Plant Foods Hum. Nutr.* **2009,** *64*, 224-229.

(63) Coghlan, M. P.; Culbert, A. A.; Cross, D. A.; Corcoran, S. L.; Yates, J. W.; Pearce, N. J.; Rausch, O. L.; Murphy, G. J.; Carter, P. S.; Roxbee Cox, L.; Mills, D.; Brown, M. J.; Haigh, D.; Ward, R. W.; Smith, D. G.; Murray, K. J.; Reith, A. D.; Holder, J. C., Selective small molecule inhibitors of glycogen synthase kinase-3 modulate glycogen metabolism and gene transcription. *Chem .Biol.* **2000,** *7*, 793-803.

(64) Bisignano, P.; Lambruschini, C.; Bicego, M.; Murino, V.; Favia, A. D.; Cavalli, A., In silico deconstruction of ATP-competitive inhibitors of glycogen synthase kinase-3beta. *J. Chem. Inf. Model.* **2012,** *52*, 3233-3244.

(65) Totrov, M.; Abagyan, R., Protein-Ligand docking as an energy optimization problem. In *Drug-receptor thermodynamics : introduction and applications*, Raffa, R. B., Ed. Wiley: Chichester ; New York, 2001; pp 603-624.

(66) Totrov, M.; Abagyan, R. In *Derivation of sensitive discrimination potential for virtual screening*, RECOMB '99. Proceedings of the Third Annual International Conference on Computational Molecular Biology, Lyon (France), ACM Press - New York: Lyon (France), 1999; pp 37-38.

(67) Bottegoni, G.; Kufareva, I.; Totrov, M.; Abagyan, R., A new method for ligand docking to flexible receptors by dual alanine scanning and refinement (SCARE). *J. Comp. Aid. Mol. Des.* **2008,** *22*, 311-325.

(68) Totrov, M.; Abagyan, R., Flexible ligand docking to multiple receptor conformations: a practical alternative. *Curr. Opin. Struct. Biol.* **2008,** *18*, 178-184.

(69) Kacker, P.; Masetti, M.; Mangold, M.; Bottegoni, G.; Cavalli, A., Combining dyad protonation and active site plasticity in BACE-1 structure-based drug design. *J. Chem. Inform. Model.* **2012,** *52*, 1079-1085.

(70) Arnautova, Y. A.; Abagyan, R. A.; Totrov, M., Development of a new physics-based internal coordinate mechanics force field and its application to protein loop modeling. *Proteins* **2011,** *79* (2), 477-498.

(71) Abagyan, R.; Raush, E.; Totrov, M. ICM Manual v.3.7. http://www.molsoft.com/man/index.html.

(72) Jia, Z.; Zhu, H.; Misra, H. P.; Li, Y., Potent induction of total cellular GSH and NQO1 as well as mitochondrial GSH by 3H-1,2-dithiole-3-thione in SH-SY5Y neuroblastoma cells and primary human neurons: protection against neurocytotoxicity elicited by dopamine, 6-hydroxydopamine, 4-hydroxy-2-nonenal, or hydrogen peroxide. *Brain Res.* **2008,** *1197*, 159-169.

TABLE OF CONTENTS GRAPHIC